MAIN-BELT ASTEROIDS OBSERVED FROM CS3: 2021 JANUARY TO MARCH

Robert D. Stephens
Center for Solar System Studies (CS3) / MoreData!
11355 Mount Johnson Ct., Rancho Cucamonga, CA 91737 USA
rstephens@foxandstephens.com

Daniel R. Coley
Center for Solar System Studies (CS3)
Corona, CA

Brian D. Warner
Center for Solar System Studies (CS3) / MoreData!
Eaton, CO

(Received: 2021 April 7)

CCD photometric observations of 24 main-belt asteroids were obtained at the Center for Solar System Studies (CS3) from 2021 January to March. In addition, 15 datasets dating back to 2013, thought to have been lost to a crashed hard drive, were recovered when a USB drive containing the reduced measurements was found. Finally, 8 pole/shape models are presented.

The Center for Solar System Studies (CS3) has nine telescopes which are normally used in program asteroid family studies. The focus is on near-Earth asteroids, but when suitable targets are not available, Jovian Trojans and Hildas are observed. When a nearly full moon is too close to the family targets being studied, targets of opportunity amongst the main-belt families were selected.

Table I lists the telescopes and CCD cameras that were used to make the observations. Images were unbinned with no filter and had master flats and darks applied. The exposures depended upon various factors including magnitude of the target, sky motion, and Moon illumination.

Telescope	Camera
0.30-m f/6.3 Schmidt-Cass	SBIG 1001E
0.35-m f/9.1 Schmidt-Cass	FLI Microline 1001E
0.35-m f/9.1 Schmidt-Cass	FLI Microline 1001E
0.35-m f/9.1 Schmidt-Cass	FLI Microline 1001E
0.35-m f/10 Schmidt-Cass	SBIG 1001E
0.35-m f/10 Schmidt-Cass	FLI Proline 1001E
0.40-m f/10 Schmidt-Cass	FLI Proline 1001E
0.40-m f/10 Schmidt-Cass	FLI Proline 1001E
0.50-m F8.1 R-C	FLI Proline 1001E

Table I: List of CS3 telescope/CCD camera combinations.

Image processing, measurement, and period analysis were done using *MPO Canopus* (Bdw Publishing), which incorporates the Fourier analysis algorithm (FALC) developed by Harris (Harris et al., 1989). For the images reduced in 2021, the Comp Star Selector feature in *MPO Canopus* was used to limit the comparison stars to near solar color. Night-to-night calibration was done using field stars from the ATLAS catalog (Tonry et al., 2018), which has Sloan *griz* magnitudes that were derived from the GAIA and Pan-STARR catalogs and are "native" magnitudes of the catalog. Those adjustments are usually ≤ ±0.03 mag. The rare greater corrections may have been related in part to using unfiltered observations, poor centroiding of the reference stars, and not correcting for second-order extinction. For the recovered measurements dating back to 2013, most used field stars from the MPOSC3 catalog, which is based on the 2MASS catalog *(http://www.ipac.caltech.edu/2mass)* but with magnitudes converted from J-K to BVRI using formulae developed by Warner (2007). The nightly zero points using this catalog have been found to be consisted to about ± 0.05 magnitude, but are occasionally higher.

The Y-axis values are ATLAS SR "sky" or Johnson V (catalog) magnitudes. The two values in the parentheses are the phase angle (a) and the value of *G* used to normalize the data to the comparison stars used in the earliest session. This, in effect, made all the observations seem to be made at a single fixed date/time and phase angle, leaving any variations due only to the asteroid's rotation and/or albedo changes. The X-axis shows rotational phase from –0.05 to 1.05. If the plot includes the amplitude, e.g., "Amp: 0.65", this is the amplitude of the Fourier model curve and *not necessarily the adopted amplitude for the lightcurve*.

For brevity, only some of the previously reported rotational periods may be referenced. A complete list is available at the asteroid lightcurve database (LCDB; Warner et al., 2009).

279 Thule. This is the first of several asteroids we were able to recover from an old crashed computer hard drive. A number of results prior to 2010 for this outer main-belt asteroid can be found in the LCDB. There is some uncertainty as to the period (Behrend, 2008web; Pravec et al., 2008web; Satō, 2015) and the suspicion of a satellite (Hamanowa and Hamanowa, 2010). We observed in 2010 (Warner et al., 2010), finding a period of 15.96 h. However, we noted due to the low amplitude the possibility of a 7.979 h period.

Subsequent to our 2010 observations, observations of Thule from 2008 by Pilcher (2014) were reported again with ambiguous periods of 7.970 h or 15.960 h. Then Marciniak et al. (2016) reported a period of 23.896 h, a 3:1 alias of the previously reported 7.9 h periods and 3:2 alias of the reported 15.9 h periods.

Our recovered 2013 data did not solve the enigmatic period. The period spectrum again shows possible periods near 8 h, 16 h, and 24 h, of near equal weighting. Because the 24 h period is commensurate with an Earth's day, a complete lightcurve cannot be obtained from a single longitude. Because the 2010 campaign involved observers from widely separated longitudes and excluded a 24 h period as a possibility, we still favor the 15.94 h period as being the most likely.

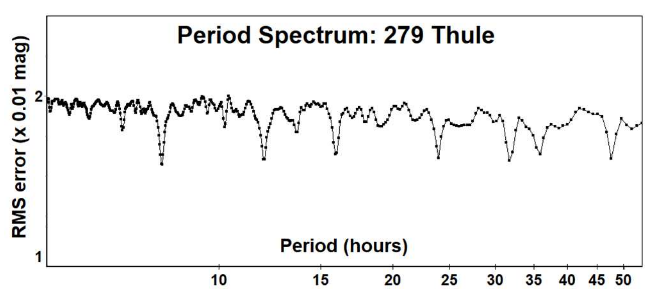

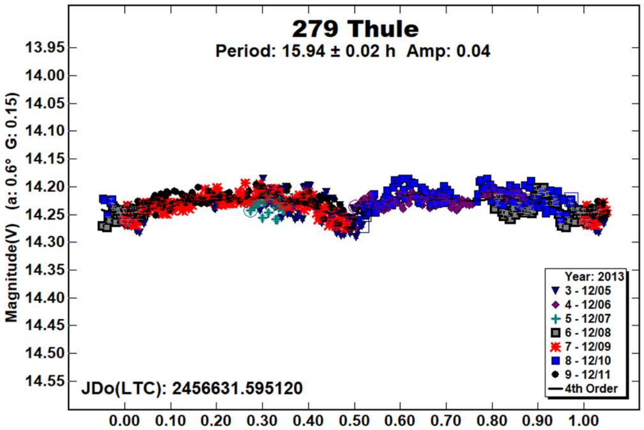

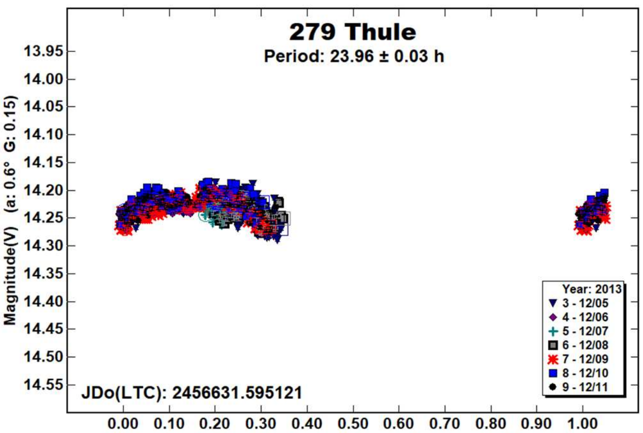

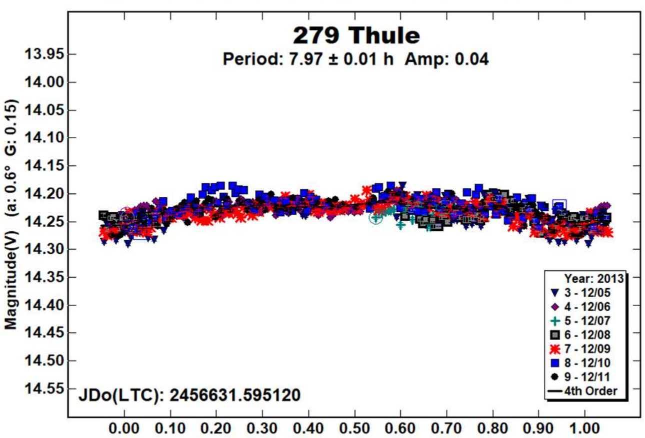

341 California. This member of the Flora family/group was another of the recovered datasets. Prior to the recovery of our data, two groups published results showing California to be a long period asteroid which was tumbling. Using observations from 2014 to 2016, Polakis and Skiff. (2017) found a primary period of 317 h with obvious signs of tumbling. Pilcher et al. (2017), using 117 sessions between 2016 June and December found a primary period of 318 h and a candidate for a secondary period of 250 h.

Our six-week run starting in 2016 January also showed signs of tumbling. Using the rules of thumb for tumbling damping time (Pravec et al., 2014; 2005), the diameter and periods make this a good candidate for tumbling. The best single period fit was 310 h. *MPO Canopus* cannot properly handle the data from a tumbling asteroid since it does not do a simultaneous search for two periods. We attempted a dual period search using the 318/250 h periods found by Pilcher et al., but the result was not an improvement over our single period search.

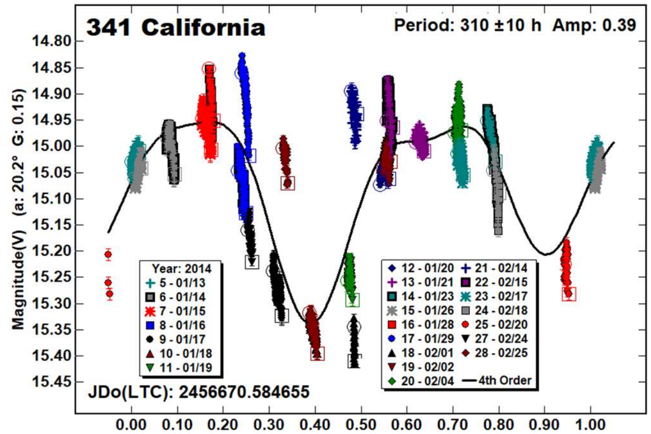

1164 Kobolda. This member of the Phocaea family/group was observed several times in the past. Higgins and Oey (2007), Sauppe et al. (2007), Higgins (2011), and Warner (2014a) each found a period near 4.14 h. Our result this year is in good agreement.

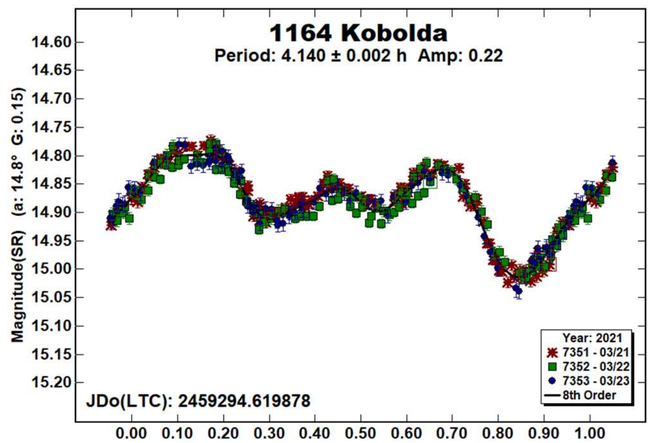

Because of the availability of the dense data from Higgins et al. and Warner in the Asteroid Lightcurve Data Exchange Format database (ALCDEF, 2020) and sparse data at the Asteroids - Dynamic web site (AstDyS-2, 2020), we attempted to solve for the sidereal period and pole position and create a shape model. These data were combined using *MPO LCInvert* (Bdw Publishing). This Windows-based program incorporates the algorithms developed by Kaasalainen and Torppa (2001) and Kaasalainen et al (2001) and converted by Josef Ďurech from the original FORTRAN to C. A period search was made over a sufficiently wide range to assure finding a global minimum in χ^2 values. We found one possible pole solution; (λ, β, P) = (270°, -61°, 4.141699 h). The full set of inversion graphics are at the end of this paper.

1331 Solvejg. This outer main-bet asteroid was observed by Garceran et al. (2016) who reported a period of 19.30 h. Using data from the Palomar Transient Factory Survey, Waszczak et al. (2015) found a period of 19.288 h. Using data from WISE and the Lowell Photometric Database, Ďurech et al. (2018a) found two possible pole solutions 180° apart: (λ, β, P) = (69°, -46°, 19.2892 h) and (248°, -41°, 19.2892 h). Their preferred solution is (69°, -46°). We recovered this dataset from 2014, finding a period of 19.33 h, consistent with those prior results.

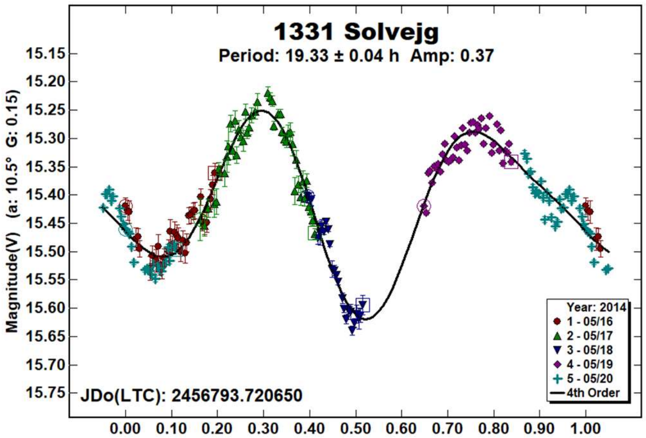

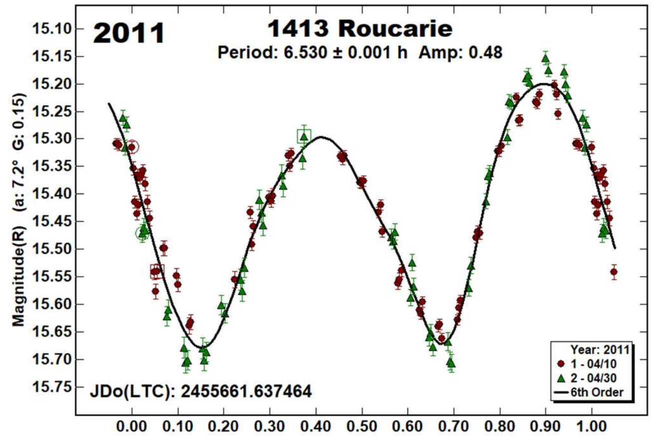

1413 Roucarie. We originally observed this member of the EOS family/group in 2011 April finding a period of 6.357 h (Coley, 2012). We observed it again in 2021 February finding a period of 6.532 h. We also recovered more data from 2013 which are consistent with the 2021 result. This caused us to revisit the 2011 period. In 2011, we only obtained two sessions, 20 days apart. Therefore, there were a many possible aliases, all of equal weight. A period of 6.530 h fits the 2011 data as well as any of the other aliases. In light of the more recent results, we are adopting that as our preferred period for the 2011 data.

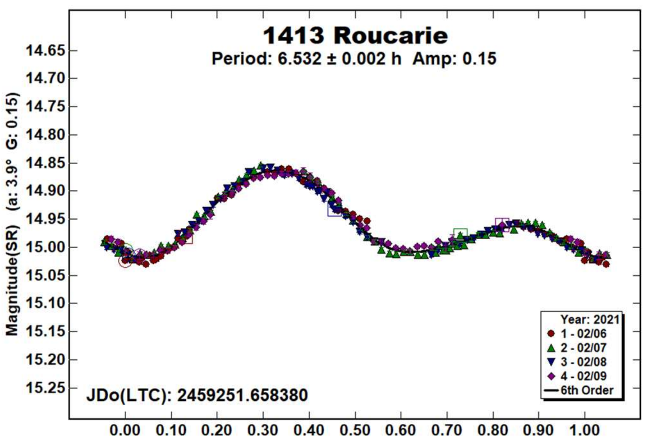

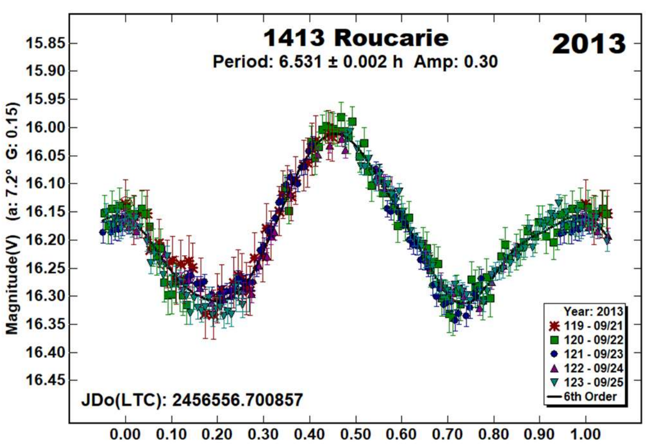

Using sparse data from the Lowell Photometric Database and WISE data, Ďurech et al. (2018a) reported a spin axis model with (λ, β) = (124°, 5°) or (310°, 5°) and a sidereal period of 6.53058 h. In addition to our dense data from the three apparitions, we used sparse data from the AstDyS-2 (2020) site to solve for the sidereal period and pole position and create a shape model.

We found two possible pols solutions 180° apart: (λ, β, *P*) = (122°, 10°, 6.530557 h) and (311°, 37°, 6.530558 h). Our preferred solution is (122°, 10°). This is in very good agreement with the Ďurech et al. model. The full set of inversion graphics are elsewhere this paper.

1568 Aisleen. This member of the Phocaea family/group was observed by Malcolm (2001) who found a period of 6.68 h. We observed it (Warner, 2014a) finding a period of 6.683 h. Finally, Behrend (2020web) reported a period of 6.6746 h. Our period this year is in good agreement with those prior results. Hanuš et al. (2011) reported a spin axis model with (λ, β) = (109°, -68°) or (310°, 5°) and a sidereal period of 6.67597 h.

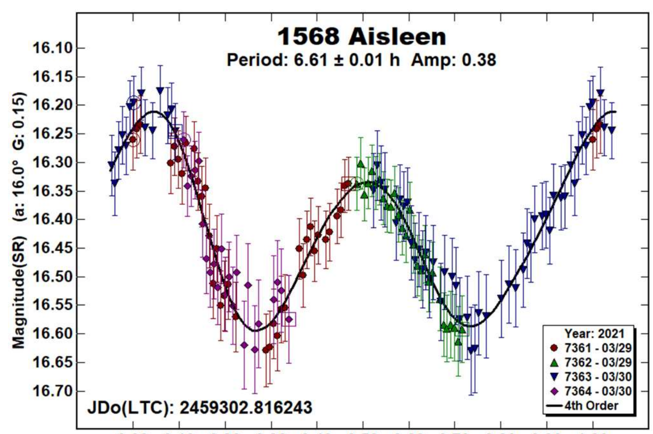

1920 Sarmiento. We have observed this member of the Hungaria family/group three times in the past (Warner, 2007; 2015; Stephens et al., 2014), each time finding a period near 4.05 h. The period we found this year is in good agreement with our prior results.

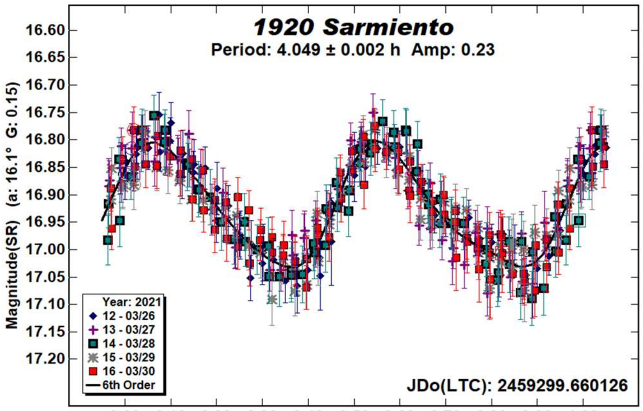

1998 Titius. We observed this Vestoid twice before (Stephens, 2016; 2017), finding periods near 6.13 h. Using data from TESS, McNeil et al. (2019) and Pál et al. (2020) found periods near 6.13 h. Our results this year are in good agreement.

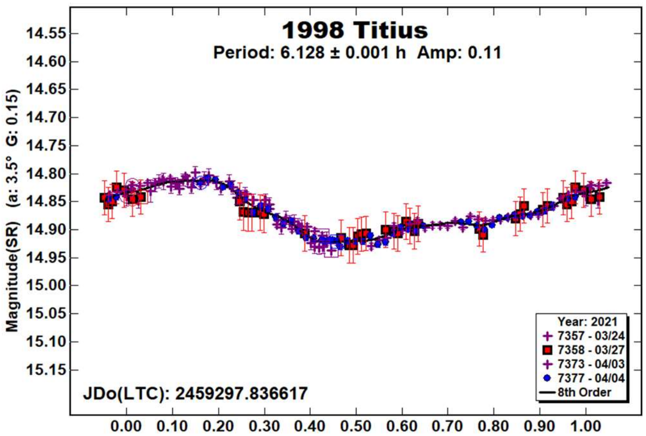

In addition to our dense data from the three apparitions, we used sparse data from the AstDyS-2 (2020) site to solve for the sidereal period and pole position and create a shape model. Our pole model showed two solutions 180° apart: (λ, β, *P*) = (236°, 2°, 6.126051 h) and (54°, 16°, 6.126052 h). Our preferred solution is (236°, 2°). The full set of inversion graphics are given elsewhere this paper.

2233 Kuznetsov. This member of the Flora family/group was observed by Ditteon and West (2011) who found a period of 5.030 h and by Stephens (2017) finding a period of 5.031 h. This year's result is in good agreement.

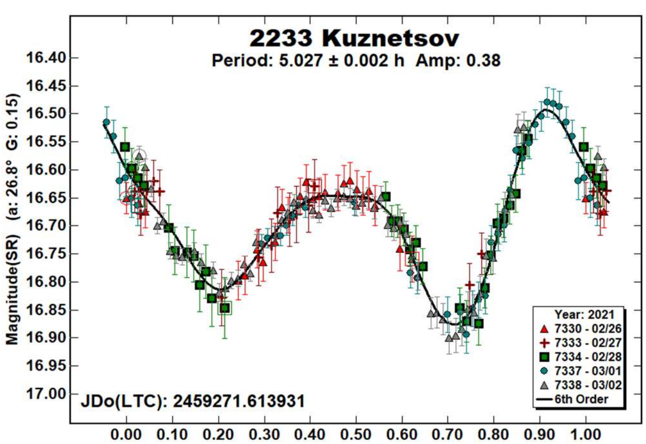

In addition to our dense data from the two apparitions, we used sparse data from the AstDyS-2 (2020) site to solve for the sidereal period and pole position and create a shape/pole model, using *MPO LCInvert* (Bdw Publishing).

Our pole model showed two possible solutions 180° apart; (λ, β, *P*) = (13°, 8°, 5.029548 h) and (192°, 1°, 5.029547 h). Our preferred solution is (13°, 8°), where the a/c ratio is 1.3 and the b/c ratio 1.2. The other solution has similar ratios.

2253 Espinette. This Mars-crosser was observed several times in the past. Behrend (2005web) reported a period of 7.440 h, Stephens (2016) reported 7.442 h, and Skiff et al. (2019) reported a period of 7.4409 h. Our result this year confirms those prior results.

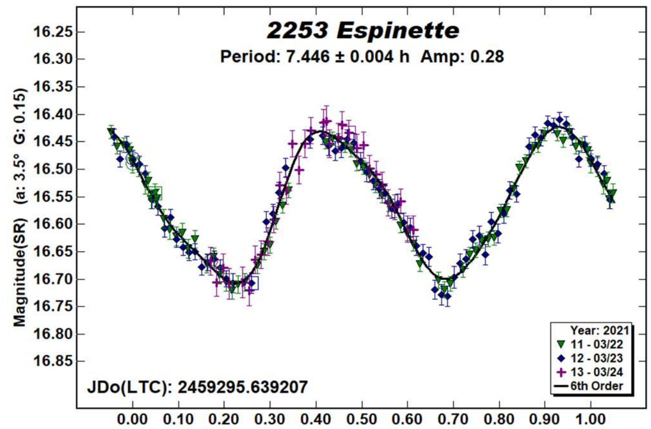

2468 Repin. This member of the Flora family/group has been observed twice in the past. We observed it (Stephens, 2016) finding a period of 4.122 h. Oey et al. (2017) did an extensive observing campaign due to its asymmetrical lightcurve, finding periods of 5.1196 h, 5.1191 h, 5.11920 h, and 5.1200 h over a four-month campaign. Our results this year is in good agreement with those prior results. In all these cases, the secondary minimum is substantially less than the primary minimum.

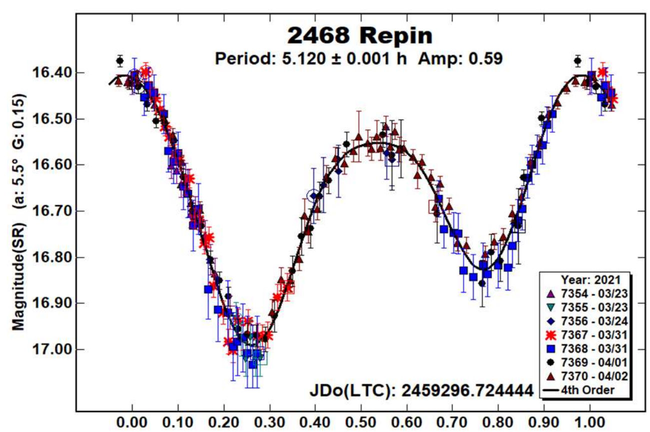

2511 Patterson. There are numerous results posted in the LCDB for this this 6 km sized member of the Vestoid family/group. Juarez et al. (2005) seems to be the first to have determined its rotational period as 4.141 h. Hasegawa et al. (2012) found a period of 4.141 h. With substantially sparser data, Waszczak et al. (2015) found a similar period. Ďurech et al. (2018b) report a sidereal period of 4.14065 h using spare and dense data. Finally, we (Stephens and Warner, 2020a) found a period of 4.139 h. The results we found this year are in good agreement.

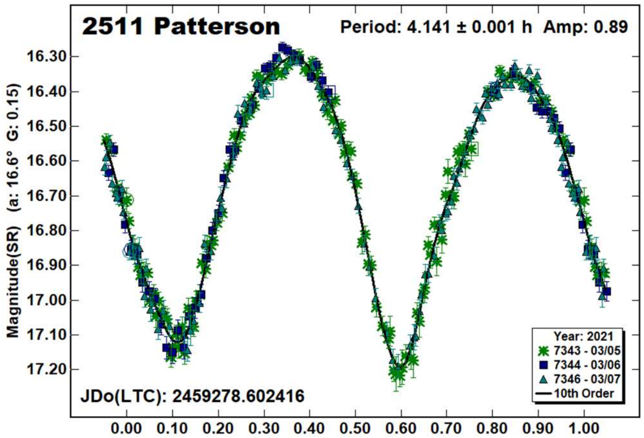

The Ďurech et al. sideral period results from a spin axis model with (λ, β) = (194°, 50°) or (10°, 31°). That model used sparse data in publicly available databases and dense data from a single night in 2016 December from the BlueEye600 robotic observatory.

In addition to our dense data from the two apparitions, we used sparse data from the AstDyS-2 (2020) site to solve for the sidereal period and pole position and to create a shape model, using *MPO LCInvert* (Bdw Publishing). We narrowed the period search based on the Ďurech et al. sideral period.

Our pole model showed two possible solutions 180° apart: (λ, β, *P*) = (215°, -80°, 4.140798 h) and (64°, -81°, 4.140797 h). Our preferred solution is (215°, -80°), where the a/c ratio is 2.75 and the b/c ratio 1.65. The other solution is similar with an a/c ratio of 2.0.

Although our sidereal period is close to the Ďurech et al. result, their latitude is substantially different, being closer to the equator. The discrepancy might result from our denser datasets, which cover seven nights over two apparitions, whereas the BlueEye600 robotic observatory was obtained on a single night. We encourage reanalysis in the future with more dense data and sparse data from ongoing surveys. The full set of inversion graphics are given at the end of this paper.

3029 Sanders. There are two periods reported in the LCDB for his member of the Flora family/group. Erasmus et al. (2020) reported a period of 3.068 h and Benishek (2020a) reported a period of 3.064 h. The period we found this year is in good agreement with those prior results.

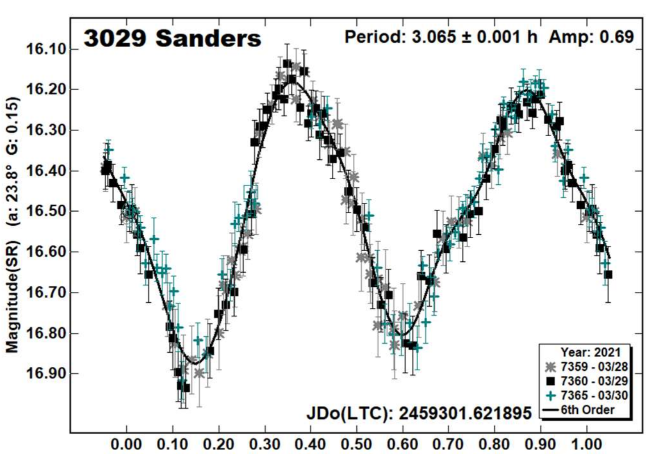

3084 Kondratyuk. This was another case of recovered data. We observed it in 2011 obtaining a partial lightcurve, by itself not sufficient to determine the period.

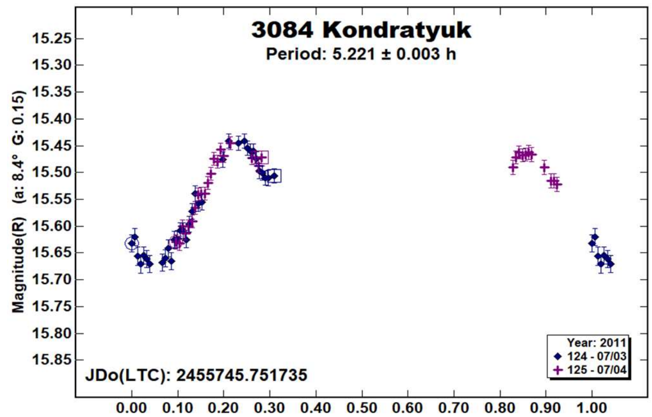

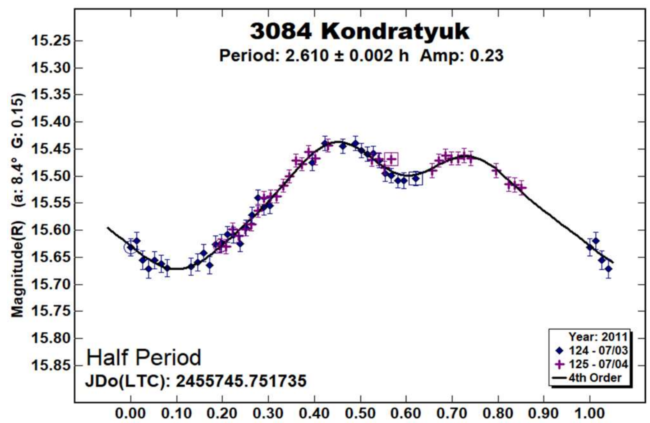

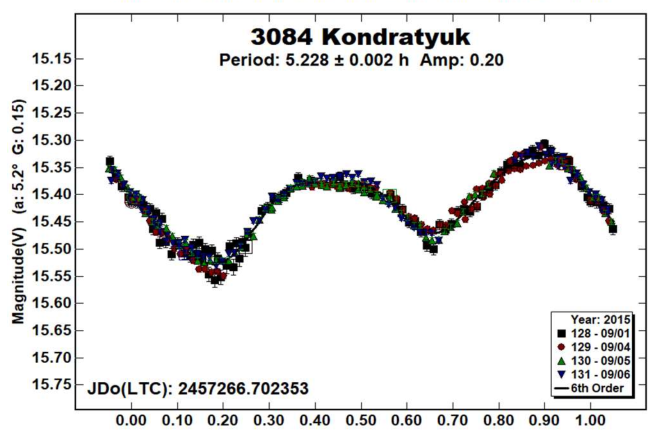

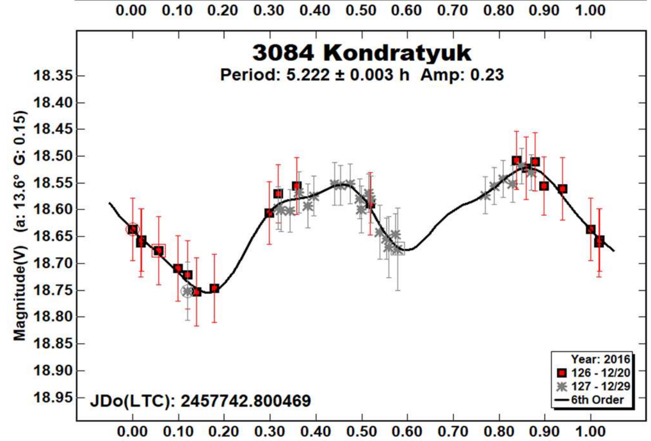

However, we were able to plot a half period of 2.610 h and therefore determine the period for the 2011 data to be 5.221 h. We reobserved it in 2015 and 2016, finding periods near 5.22 h. We plotted the 2011 data to the periods found in 2015 and 2016.

3198 Wallonia. This Mars-crosser has periods reported in the LCDB three times in the past (Behrend, 2005web, 7.58 h; Warner, 2008, 7.54 h; Stephens, 2018, 7.569 h). Our result this year is in good agreement with the previous results.

Using our prior dense datasets from 2008 and 2018 and sparse data at the Asteroids - Dynamic web site (AstDyS-2, 2020), we attempted to solve for the sidereal period and pole position and to create a shape model. A period search was made over a sufficiently wide range to assure finding a global minimum in χ^2 values.

Our pole model showed two possible solutions 180° apart: (λ, β, P) = (115°, -47°, 7.565854 h) and (253°, -45°, 7.565858 h). Our preferred solution is (115°, -47°). The full set of inversion graphics are given at the end of this paper.

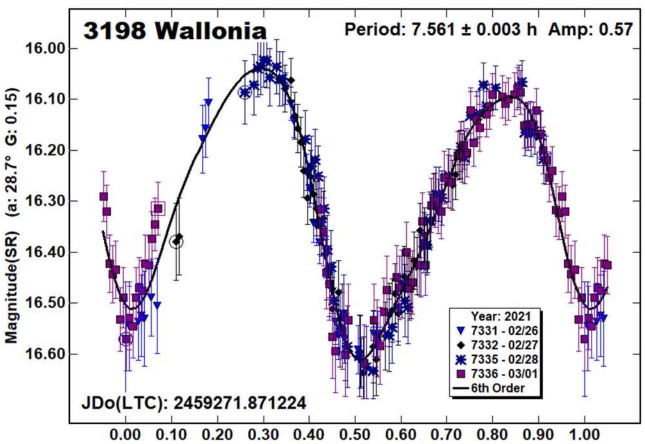

3248 Farinella. This outer main-belt asteroid has been observed many times. Ditteon et al. (2012) originally found a period of 6.676 h. However, upon reobservation, Ditteon et al. (2019) concluded a half period of 3.339 h was a better fit. Using data from TESS, Pál et al. (2020) found a period of 6.6749 h. Our result this year is a good match to the original Ditteon et al. period and the Pál et al. result.

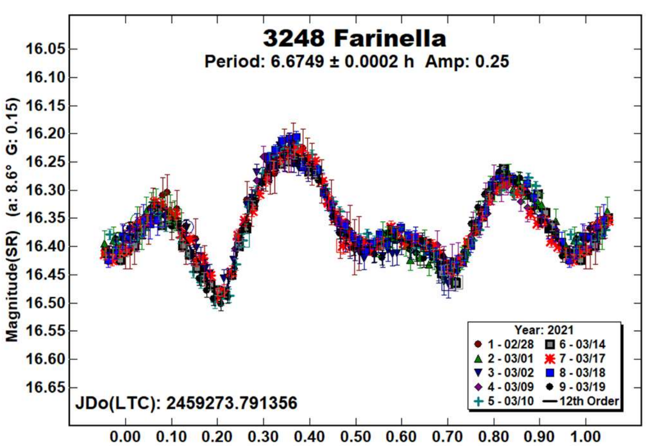

3339 Treshnikov. This outer main-belt asteroid was last observed in 2012 June (Owings, 2013), who found a period of 18.2947 h. We were able to recover this data from 2017, which is consistent with the Owings result.

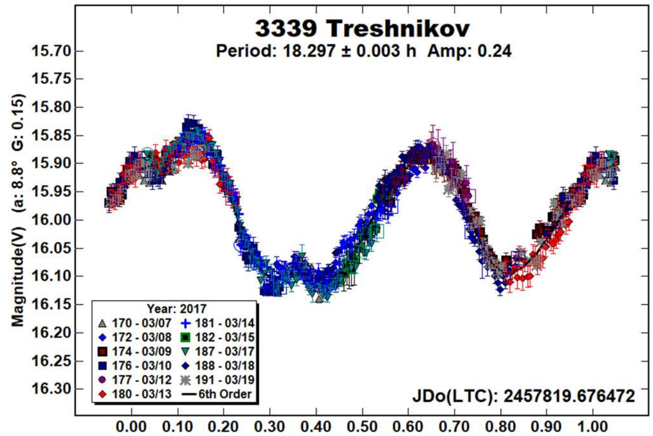

3506 French. This member of the EOS family/group was another 'dusty file cabinet' find, having been observed in 2013 October. Later, Waszczak et al. (2015) reported a period of 16.756 h using sparse data from the Palomar Transient Factory Survey. The Waszczak et al. data was coincidently obtained two weeks after our data. Our denser data and 14th order lightcurve resulted in an amplitude 0.3 magnitude higher than the Waszczak et al. result, which only used two orders in their analysis.

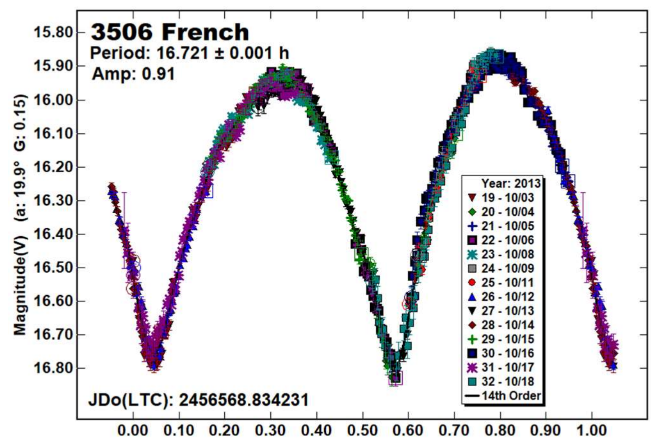

5040 Rabinowitz. This member of the Phocaea family/group was observed three times in the past. Pravec (2013web) reported a period of 4.6901 h. We observed it in 2013 (Stephens and Coley, 2013) finding a period of 4.691 h.

Finally, Clark (2014) observed it in 2013 finding a period of 4.472 h. The Clark observations were obtained over a six-week span and showed substantial changes in the amplitude of the lightcurve, perhaps explaining the difference in the rotational period from the other results. These data from 2016 were part of the recovered dataset. The period we found for 2016 agrees with Pravec's and our previous result.

Because of our dense data, and the availability of some dense data from Klinglesmith in the Asteroid Lightcurve Data Exchange Format database (ALCDEF, 2020) and sparse data at the Asteroids - Dynamic web site (AstDyS-2, 2020), we attempted to solve for the sidereal period and pole position and to create a shape model. We found one possible pole: (λ, β, P) = (101°, 48°, 4.690155 h).

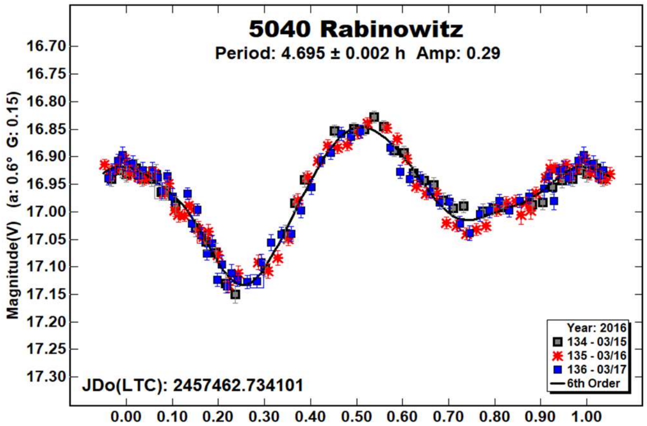

[5096 Luzin]. This Vestoid has been observed three times in the past; Klinglesmith et al. (2013), Benishek (2020b), and Stephens and Warner (2020b), each time finding a rotational period near 3.05 h. The result we found this year is in good agreement.

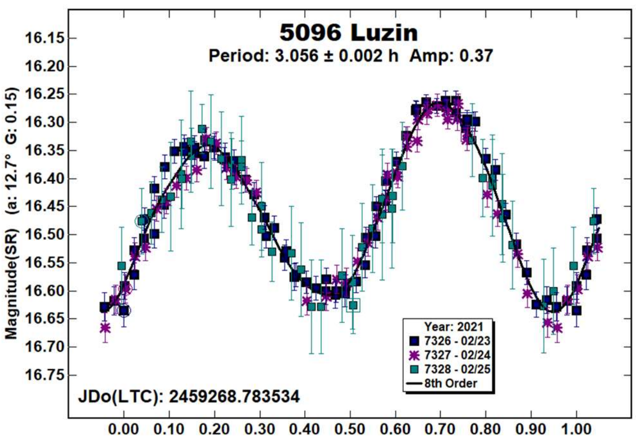

Because of the availability of the Klinglesmith et al. and Benishek data in the Asteroid Lightcurve Data Exchange Format database (ALCDEF, 2020), sparse data at the Asteroids - Dynamic web site (AstDyS-2, 2020), and our dense data from two apparitions, we attempted to solve for the sidereal period and pole position and to create a shape model.

Our pole model showed two possible solutions 180° apart: (λ, β, P) = (75°, 54°, 3.054594 h) and (249°, 35°, 3.054594 h). Our preferred solution is (75°, 54°).

[(5747) 1991 CO3]. Our recovered data files included this member of the Phocaea family. We observed it once before (Warner, 2009) reporting a period of 38.6 h with an amplitude of 0.30 mag. That lightcurve had only partial coverage from six sessions over 14 nights. This much more complete dataset has 23 sessions spanning a month. Several of those sessions have an amplitude exceeding the amplitude of our original lightcurve. Although the magnitudes at the time were determined using field stars converted to approximate Johnson V magnitudes based on 2MASS J-K colors (Warner, 2007), very few zero-point adjustments were needed to determine the period to be 196.45 h. With this in mind, we reanalyzed our 2008 dataset. We found many zero-point adjustments were applied to the nightly sessions. Upon removing those, we found a large amplitude, slowly rotating asteroid. The 2008 run was not long enough complete the lightcurve, but we were able to determine the half period, which gives us a period of 197.9 h.

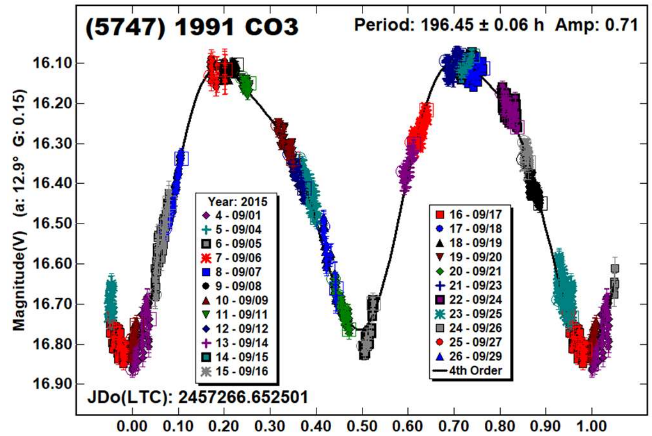

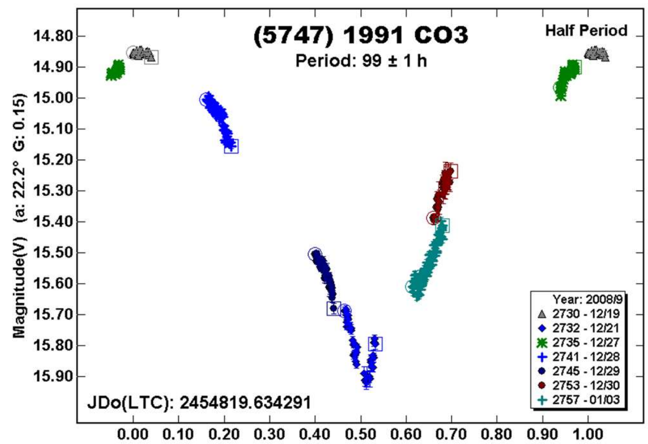

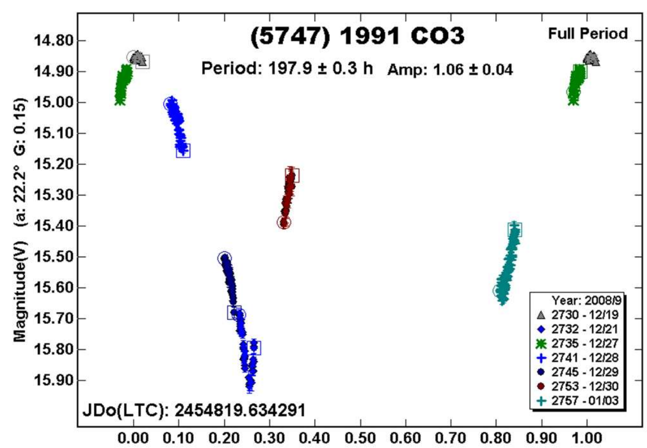

Although this asteroid is a good candidate for tumbling according to the rules of thumb for tumbling damping time (Pravec et al., 2014; 2005), there are no obvious signs of tumbling in either the 2008 or 2016 lightcurves.

[6859 Datemasamune]. It has always been a problem determining the rotational period of this member of the Hungaria family/group because its amplitude never exceeds 0.12 mag. We observed Datemasamune in 2006, 2009, 2011, 2016, and 2019 (Stephens and Warner, 2019 and references therein), resulting in an ambiguous lightcurve with possible periods between 5.90 h and 9.95 h, with 5.944 h being our preferred period. We recovered additional data from 2014, which did not solve the discrepancy. With only three nights of data from 2014, the period error spans most of these possible periods.

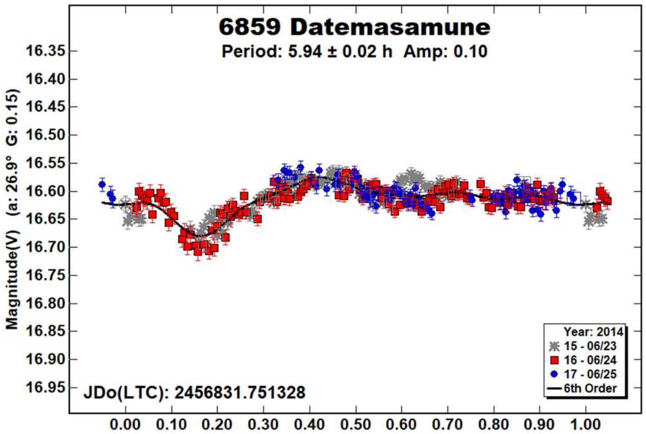

6901 Roybishop. We observed this member of the Hungaria family/group in 2008, 2011, 2015, and 2019 (Stephens and Warner, 2020a and references therein), finding ambiguous solutions as a result of its low amplitude (0.04-0.09 mag.) lightcurves. We subsequently recovered more data from 2016, which did not solve the ambiguity. Although our preferred period of 4.766 h agrees with our 2019 results, it is only a partial lightcurve. Our alternative 2019 result of 9.533 h still cannot be ruled out.

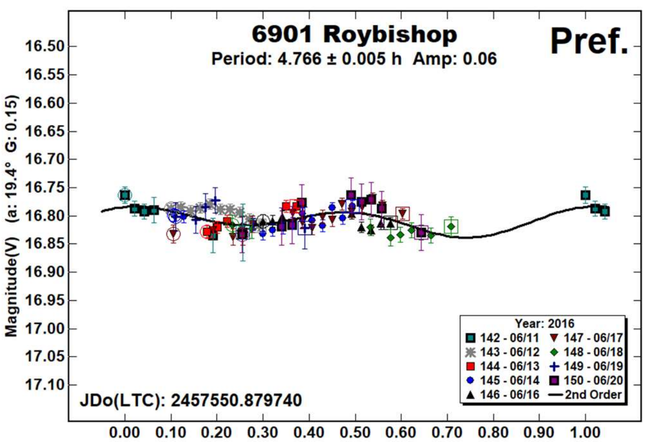

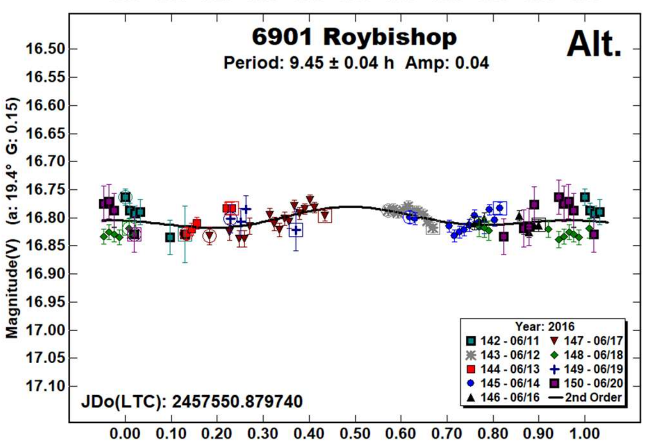

7660 Alexanderwilson. We observed this member of the Hungaria family/group four times in the past (Stephens et al., 2014; Warner, 2012a; 2014b; 2016), each time finding a period near 5.92 h. We recovered data from 2016, which led to a period that is in good agreement with the previous results. Hanuš et al. (2018) reported a spin axis model with (λ, β, *P*) = (321°, 15°) and a sidereal period of 5.91818 h.

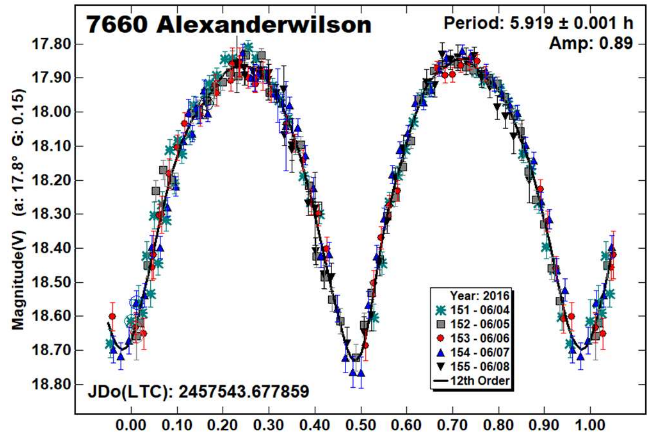

(15123) 2000 EP36. We could not find any periods posted in the LCDB for this member of the Themis family/group. This was another recovered dataset from 2017.

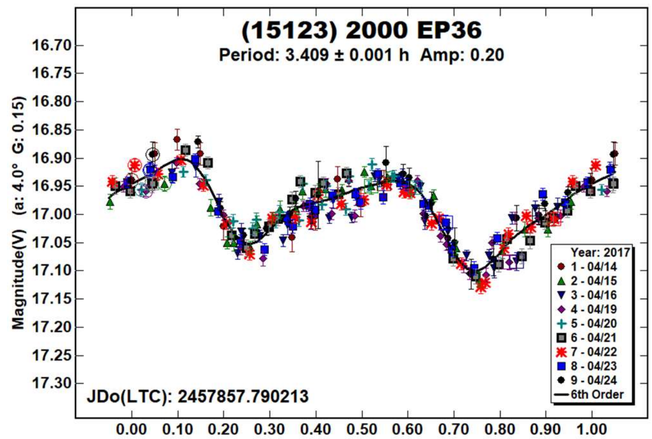

17823 Bartels. This inner main-belt asteroid was observed by the Palomar Transient Factory Survey (Waszczak et al., 2015) who found a period of 3.800 h. Pál el al. (2020), using data from TESS, found a period pf 11.3946 h. We were able to recover much denser datasets from 2013 which shows the period to be 3.784 h, close to the sparser Palomar data.

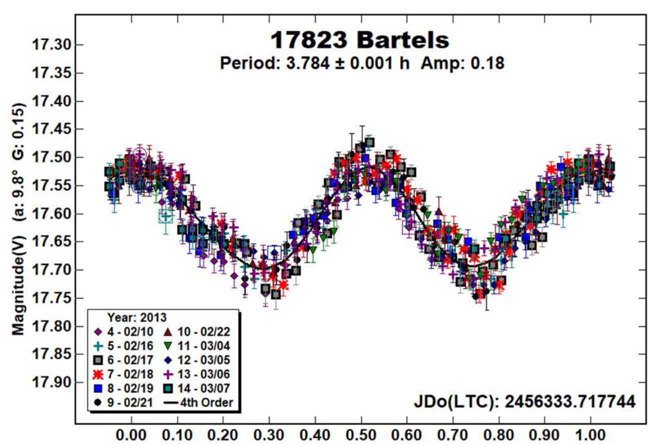

(19979) 1989 VJ. Han et al. (2013) reported a period of 7.568 h for this Vestoid. Our result this year is in good agreement.

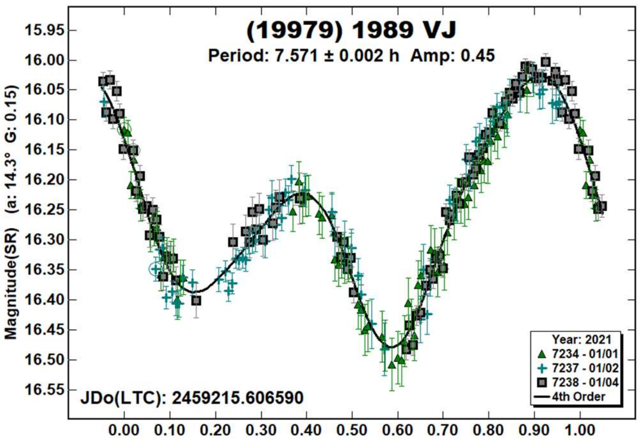

(26895) 1995 MC. We could not find any periods posted in the LCDB for this outer main-belt asteroid. This dataset was recovered from 2012. This target was followed for a month due to its low amplitude and period being commensurate with one half an Earth's day.

The solution produced a bimodal lightcurve, but the period spectrum shows the possibility of a monomodal or quadrimodal lightcurve. Given the relatively low and amplitude, a bimodal solution is not assured (Harris et al., 2014).

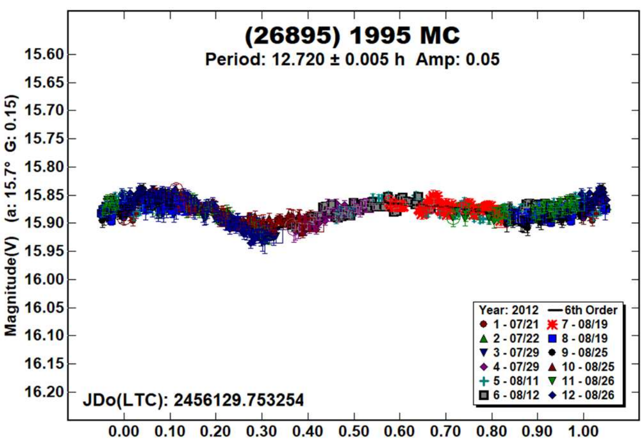

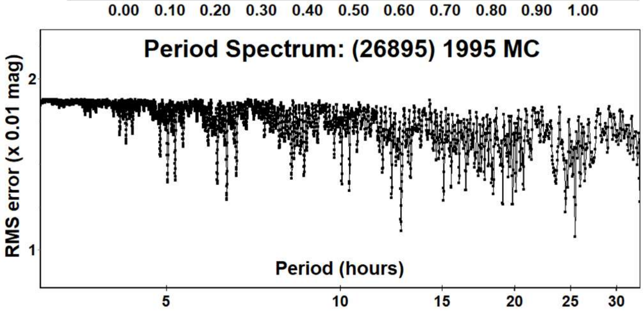

(27011) 1998 FU22. There are no entries in the LCDB for this member of the Flora family/group. It was a target of opportunity in the field of (7458) 1984 DE1 for only three nights. The slope of the individual nights suggests a long period asteroid. There were insufficient data to definitely find a period, but a half period of 37 h points to a full period of 73.4 h.

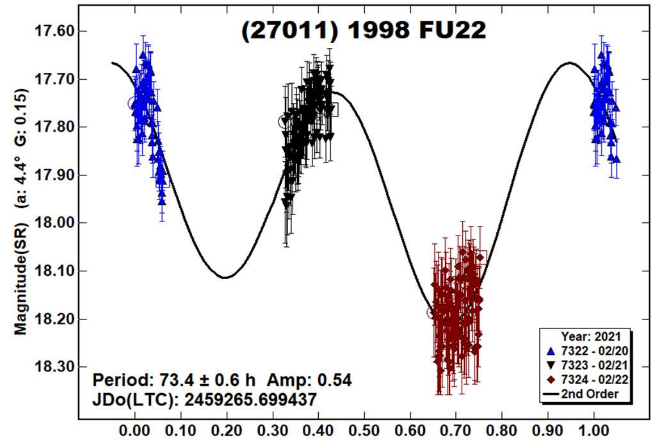

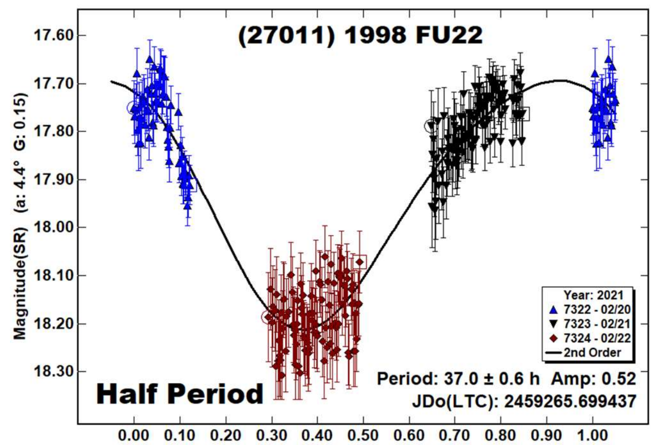

(30781) 1988 CR2. This member of the Flora family/group was observed by Chang et al. (2015) and Waszczak et al. (2015) using the Palomar Transient Factory Survey, each finding periods near 5.82 h. We recovered this dense data from 2015, finding a period near those prior results.

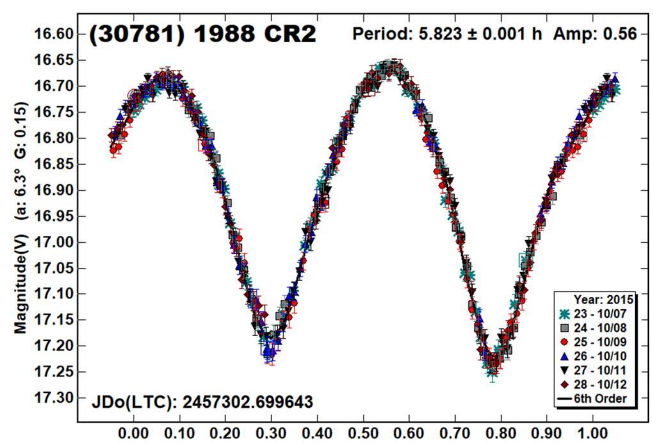

34817 Shiominemoto. We have observed this member of the Hungaria family/group four times in the past (Warner, 2007; 2011; 2012b; Stephens, 2015), each time finding a period near 6.38 h. We recovered this data from 2016, which produced a period that is in good agreement with our prior results. Ďurech et al. (2018b) reported a spin axis model with (λ, β, P) = (201°, 36°, 6.37750 h).

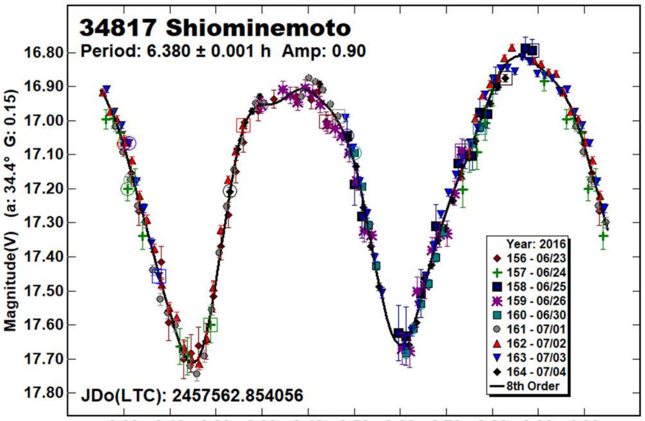

(35194) 1994 ET3. We observed this member of the Hungaria family/group once in the past (Stephens et al., 2014) finding a period of 8.912 h. Since then, we have recovered observations from 2016 and 2019. Along with our new 2021 results, all have a rotational period in good agreement with the 2014 result.

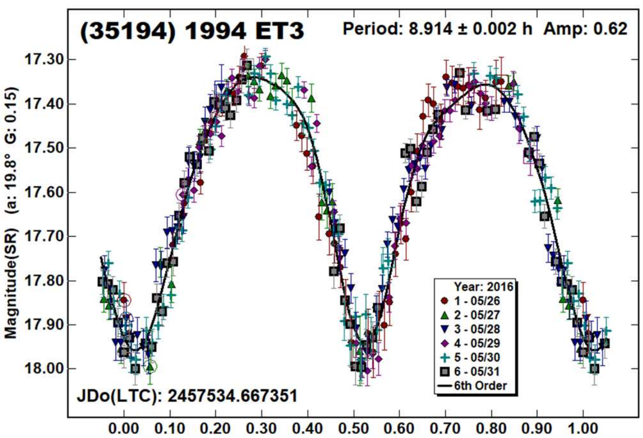

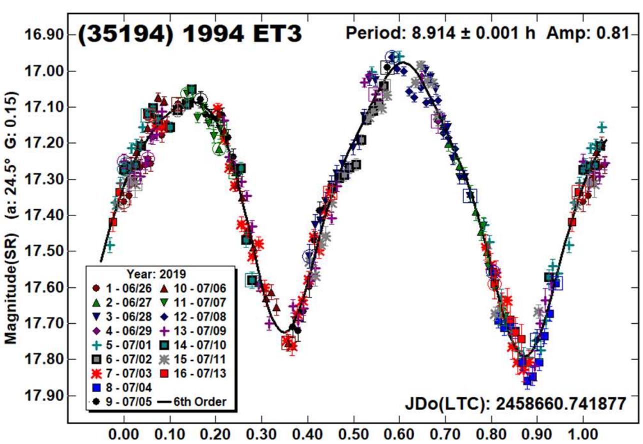

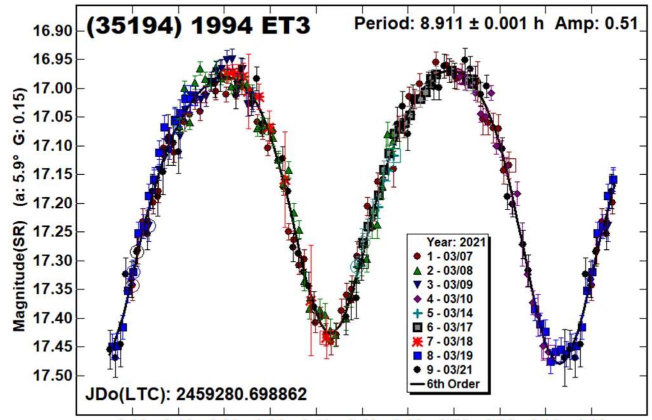

(45068) 1999 XA34. This member of the EOS family/group was observed by Waszczak et al. (2015) using the Palomar Transient Factory Survey, finding a period of 5.043 h. Our result this year is in agreement.

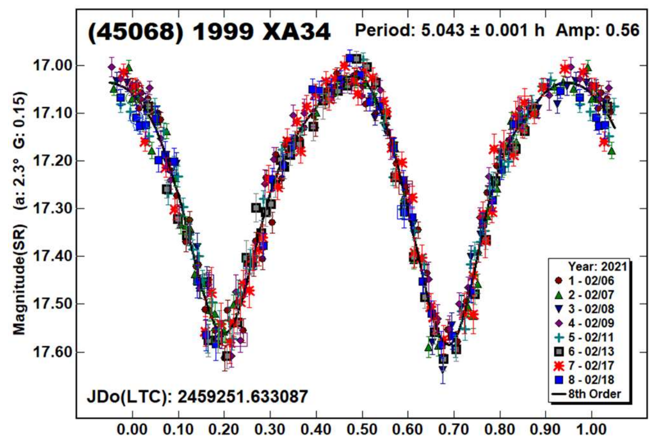

(46598) 1993 FT2. This Mars-crosser was observed in 2007 by Pray et al. (2008) who found a period of 4.86 h. Our result this year is in good agreement.

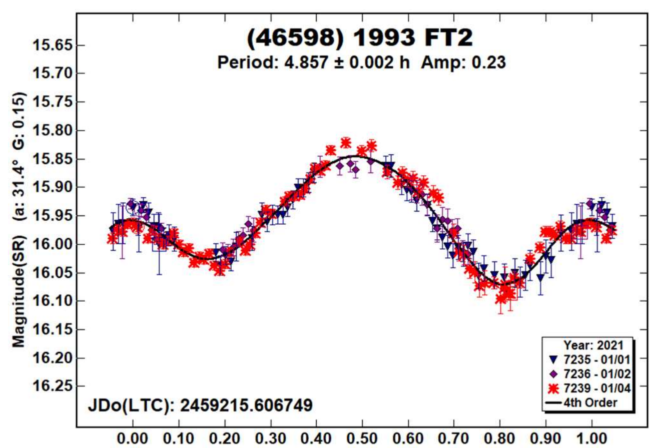

169078 Chuckshaw. There are no entries in the LCDB for this member of the Eunomia family/group. This was another set of recovered data originally obtained in 2014 May.

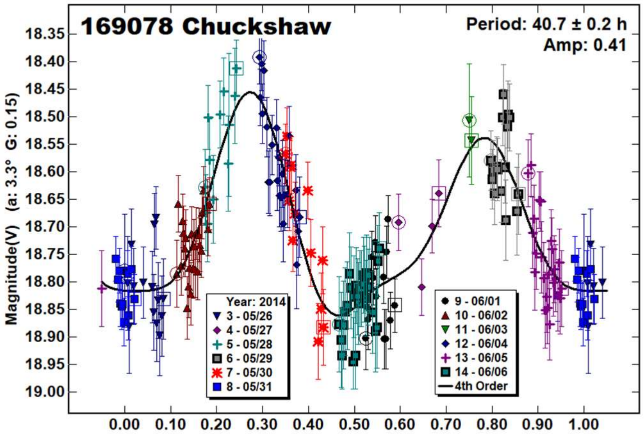

Acknowledgements

Observations at CS3 and continued support of the asteroid lightcurve database (LCDB; Warner et al., 2009) are supported by NASA grant 80NSSC18K0851.

This work includes data from the Asteroid Terrestrial-impact Last Alert System (ATLAS) project. ATLAS is primarily funded to search for near earth asteroids through NASA grants NN12AR55G, 80NSSC18K0284, and 80NSSC18K1575; byproducts of the NEO search include images and catalogs from the survey area. The ATLAS science products have been made possible through the contributions of the University of Hawaii Institute for Astronomy, the Queen's University Belfast, the Space Telescope Science Institute, and the South African Astronomical Observatory.

The authors gratefully acknowledge Shoemaker NEO Grants from the Planetary Society (2007, 2013). These were used to purchase some of the telescopes and CCD cameras used in this research.

References

ALCDEF (2020). Asteroid Lightcurve Data Exchange Format database. *http://www.alcdef.org/*

AstDys-2 (2020). Asteroids - Dynamic site. *https://newton.spacedys.com/astdys/*

Behrend, R., (2005web, 2008web, 2020web). Observatoire de Geneve web site. *http://obswww.unige.ch/~behrend/page_cou.html*

Benishek, V. (2020a). "Asteroid Photometry at Sopot Astronomical Observatory: 2019 June-October." *Minor Planet Bull.* **47**, 75-83.

Benishek, V. (2020b). "Photometry of 39 Asteroids at Sopot Astronomical Observatory: 2019 September - 2020 March." *Minor Planet Bull.* **47**, 231-241.

Chang, C.-K., Ip, W.-H., Lin, H.-W., Cheng, Y.-C., Ngeow, C.-C., Yang, T.-C., Waszczak, A., Kulkarni, S.R., Levitan, D., Sesar, B., Laher, R., Surace, J., Prince, T.A. (2015). "Asteroid Spin-rate Study Using the Intermediate Palomar Transient Factory." *Ap. J. Suppl. Ser.* **219**, A27.

Clark, M. (2014). "Asteroid Photometry from the Preston Gott Observatory." *Minor Planet Bull.* **41**, 100-101.

Coley, D. (2012). "Asteroid Lightcurve Analysis at the Danhenge Observatory Apr - Aug 2011." *Minor Planet Bull.* **39**, 13-24.

Ditteon, R.; West, J. (2011). "Asteroid Lightcurve Analysis at the Oakley Southern Observatory: 2011 January thru April." *Minor Planet Bull*. **38**, 214-217.

Ditteon, R.; Horn, L.; Kamperman, A.; Vorjohan, B.; Kirkpatrick, E. (2012). "Asteroid Lightcurve Analysis at the Oakley Souther Sky Observatory: 2011 April-May." *Minor Planet Bull.* **39**, 26-28.

Ditteon, R.; Johnson, D.; Lin, W.; Wang, Z.; Zhao, B. (2019). "Lightcurve Analysis of Minor Planets Observed at the Oakley Southern Sky Observatory: 2018 August-September." *Minor Planet Bull.* **46**, 280-282.

Ďurech, J.; Hanuš, J.; Alí-Lagoa, V. (2018a). "Asteroid models reconstructed from the Lowell Photometric Database and WISE data." *Astron. Astrophys*. **617**, A57.

Ďurech, J.; Hanuš, J.; Broz, M.; Lehky, M.; Behrend, R.; Antonini, P.; Charbonnel, S.; Crippa, R.; Dubreuil, P.; Farroni, G.; Kober, G.; Lopez, A.; Manzini, F.; Oey, J.; Poncy, R.; Rinner, C.; Roy, R. (2018b). "Shape models of asteroids based on lightcurve observations with BlueEye600 robotic observatory." *Icarus* **304**, 101-109.

Erasmus, N.; Navarro-Meza, S.; McNeill, A.; Trilling, D.E.; Sickafoose, A.A.; Denneau, L.; Flewelling, H.; Heinze, A.; Tonry, J.L. (2020). "Investigating Taxonomic Diversity within Asteroid Families through ATLAS Dual-band Photometry." *Ap. J.* **247***,* A13.

Garceran, A.C.; Aznar, A.; Mansego, E.A.; Rodriguez, P.B.; de Haro, J.L.; Silva, A.F.; Silva, G.F.; Martinez, V.M.; Chiner, O.R. (2016). "Nineteen Asteroids Lightcurves at Asteroids Observers (OBAS) - MPPD: 2015 April - September." *Minor Planet Bull*. **43**, 92-97.

Hamanowa, H., Hamanowa, H. (2010). Hamanowa Astronomical Obs. Web site. *http://www2.ocn.ne.jp/~hamaten/astcjata.htm*

Han, X.L.; Li, B.; Zhao, H.; Liu, W.; Sun, L.; Shi, J.; Gao, S.; Wang, S.; Pan, X.; Jiang, P.; Zhou, H. (2013). "Photometric Observations of 782 Montefiore, 3842 Harlansmith 5542 Moffatt, 6720 Gifu, and (19979) 1989 VJ." *Minor Planet Bull*. **40**, 99-100.

Hanuš, J.; Ďurech, J.; Brož, M.; Warner, B.D.; Pilcher, F.; Stephens, R.; Oey, J.; Bernasconi, L.; Casulli, S.; Behrend, R.; Polishook, D.; Henych, T.; Lehký, M.; Yoshida, F.; Ito, T. (2011). "A study of asteroid pole-latitude distribution based on an extended set of shape models derived by the lightcurve inversion method." *Astron. Astrophys.* **530**, A134.

Hanuš, J.; Ďurech, J.; Oszkiewicz, D.A.; Behrend, R.; Carry, B.; Delbo, M.; Adam, O.; Afonina, V.; Anquetin, R.; Antonini, P.; Arnold, L.; Audejean, M.; Aurard, P.; Bachschmidt, M.; Baduel, B.; Barbotin, E.; Barroy, P.; Baudouin, P.; Berard, L.; Berger, N. (2018). "New and updated convex shape models of asteroids based on optical data from a large collaboration network." *Astron. Astrophys.* **586**, A108.

Harris, A.W.; Young, J.W.; Scaltriti, F.; Zappala, V. (1984). "Lightcurves and phase relations of the asteroids 82 Alkmene and 444 Gyptis." *Icarus* **57**, 251-258.

Number	Name	21yy/mm/dd	Phase	L_{PAB}	B_{PAB}	Period(h)	P.E.	Amp	A.E.	Grp
279	Thule	13/12/05-12/11	0.6,2.2	71		15.94	0.02	0.04	0.02	MB-O
						7.97	0.03	0.04	0.02	
						23.96	0.03			
341	California	14/01/13-02/25	20.2,24.4	72	5	310	10	0.43	0.10	FLOR
1164	Kobolda	03/21-03/23	14.8,15.9	160	7	4.140	0.002	0.22	0.02	PHO
1331	Solvejg	05/16-05/20	10.5,11.8	208	4	19.33	0.04	0.37	0.02	MB-O
1413	Roucarie	11/04/10-04/30	7.3,13.7	182	2	6.530	0.001	0.48	0.02	MB-O
		13/09/21-09/25	7.3,8.5	339	3	6.531	0.002	0.30	0.02	
		02/06-02/09	3.9,4.3	135	-9	6.532	0.002	0.15	0.01	
1568	Aisleen	03/29-03/30	16.0,15.9	224	28	6.61	0.01	0.38	0.02	PHO
1920	Sarmiento	03/26-03/30	16.1,16.2	184	28	4.049	0.002	0.23	0.02	H
1998	Titius	03/24-04/04	*3.5,3.3	189	-3	6.128	0.001	0.11	0.02	V
2233	Kuznetsov	02/26-03/02	26.8,27.0	91	-2	5.027	0.002	0.38	0.02	FLOR
2253	Espinette	03/22-03/24	3.7,4.6	174	3	7.446	0.004	0.28	0.02	MC
2468	Repin	03/23-04/02	5.6,9.8	172	-5	5.120	0.001	0.59	0.02	FLOR
2511	Patterson	03/05-03/07	16.6,17.2	129	8	4.141	0.001	0.89	0.02	V
3029	Sanders	03/28-03/30	23.8,24.3	140	-1	3.065	0.001	0.69	0.02	FLOR
3084	Kondratyuk	11/07/03-07/04	*9.1,8.6	293	6	5.221	0.003	0.23	0.02	MB-I
		15/09/01-09/06	5.2,2.4	345	2	5.228	0.002	0.20	0.02	MB-I
		16/12/20-12/29	13.6,10.7	125	-5	5.222	0.003	0.23	0.03	
3198	Wallonia	02/26-03/01	28.7,28.0	205	23	7.561	0.003	0.57	0.03	MC
3248	Farinella	02/28-03/19	8.6,12.5	132	10	6.6749	0.0002	0.25	0.02	MB-O
3339	Treshnikov	17/03/07-03/19	8.8,11.1	157	21	18.297	0.003	0.24	0.03	MB-O
3506	French	13/10/03-10/18	19.9,17.2	69	10	16.721	0.001	0.91	0.02	EOS
5040	Rabinowitz	03/15-03/17	*0.6,0.4	176	0	4.695	0.002	0.29	0.02	PHO
5096	Luzin	02/23-02/25	12.8,11.9	180	-5	3.056	0.002	0.37	0.02	V
5747	1991 CO3	08/12/19-01/03	*22.6,26.8	59	20	197.9	0.3	1.05	0.10	PHO
		15/09/01-09/29	*12.8,18.0	337	28	196.45	0.06	0.71	0.02	
6859	Datemasamune	14/12/31-12/31	*26.9,26.3	306	23	5.94	0.02	0.10	0.02	H
6901	Roybishop	16/06/11-06/20	19.5,15.5	294	0	4.766	0.005	0.06	0.02	H
						9.45	0.01	0.06	0.02	
7660	Alexanderwilson	16/06/04-06/08	17.8,17.8	258	32	5.919	0.001	0.89	0.02	H
15123	2000 EP36	17/04/14-04/24	4.0,8.1	195	1	3.409	0.001	0.20	0.02	MB-O
17823	Bartels	13/02/10-03/07	*9.8,5.5	158	5	3.784	0.001	0.18	0.02	MB-I
19979	1989 VJ	01/01-01/04	14.4,15.6	74	0	7.571	0.002	0.45	0.02	V
26895	1995 MC	07/21-08/12	15.7,8.1	327	10	12.720	0.005	0.05	0.02	MB-M
27011	1998 FU22	02/20-02/22	*4.5,3.0	160	-1	73.4	0.6	0.54	0.10	FLOR
30781	1988 CR2	10/07-10/12	6.3,7.8	10	-9	5.823	0.001	0.56	0.02	FLOR
34817	Shiominemoto	06/23-07/04	34.4,33.0	328	14	6.380	0.001	0.90	0.02	MC
35194	1994 ET3	16/05/26-05/31	*19.8,20.4	241	34	8.914	0.002	0.62	0.02	H
		19/06/26-07/13	24.4,23.1	304	26	8.914	0.001	0.81	0.02	
		03/07-03/21	*5.9,6.8	174	8	8.911	0.001	0.51	0.02	
45068	1999 XA34	02/06-02/18	2.3,7.0	132	1	5.043	0.001	0.56	0.02	EOS
46598	1993 FT2	01/01-01/04	31.4,32.0	62	29	4.857	0.002	0.23	0.02	MC
169078	Chuckshaw	05/26-06/06	*3.3,3.1	250	-2	40.7	0.2	0.41	0.05	MB-M

Table III. Observing circumstances and results. The phase angle is given for the first and last date. If preceded by an asterisk, the phase angle reached an extrema during the period. L_{PAB} and B_{PAB} are the approximate phase angle bisector longitude/latitude at mid-date range (see Harris et al., 1984). Grp is the asteroid family/group (Warner et al., 2009): ERI, Erigone; EUN, Eunomia; FLOR, Flora; H, Hungaria; KOR, Koronis; MC, Mars-crosser; PHO, Phocaea.

Harris, A.W.; Young, J.W.; Contreiras, L.; Dockweiler, T.; Belkora, L.; Salo, H.; Harris, W.D.; Bowell, E.; Poutanen, M.; Binzel, R.P.; Tholen, D.J.; Wang, S. (1989). "Phase relations of high albedo asteroids: The unusual opposition brightening of 44 Nysa and 64 Angelina." *Icarus* **81**, 365-374.

Harris, A.W., Pravec, P., Galad, A., Skiff, B.A., Warner, B.D., Vilagi, J., Gajdos, S., Carbognani, A., Hornoch, K., Kusnirak, P., Cooney, W.R., Gross, J., Terrell, D., Higgins, D., Bowell, E., Koehn, B.W. (2014). "On the maximum amplitude of harmonics on an asteroid lightcurve." *Icarus* **235**, 55-59.

Hasegawa, S.; Miyasaka, S.; Mito, H.; Sarugaku, Y.; Ozawa, T.; Kuroda, D.; Nishihara, S.; Harada, A.; Yoshida, M.; Yanagisawa, K.; Shimizu, Y.; Nagayama, S.; Toda, H.; Okita, K.; Kawai, N.; Mori, M.; Sekiguchi, T.; Ishiguro, M.; Abe, M. (2012). "Lightcurve Survey of V-Type Asteroids. Observations Until 2005." *ACM 2012, Proceedings of the conference held May 16-20, 2012* Id. 6281.

Higgins, D.; Oey, J. (2007). "Asteroid Lightcurve Analysis at Hunters Hill Observatory and Collaborating Stations - December 2006 - April 2007." *Minor Planet Bull.* **34**, 79-80.

Higgins, D. (2011). "Period Determination of Asteroid Targets Observed at Hunters Hill Observatory: May 2009 - September 2010." *Minor Planet Bull.* **38**, 41-46.

Juarez, R.A.; Martinez, C.T.; Ryan, W.H.; Ryan, E.V. (2005). "Physical Properties of the Vesta family asteroid 2511 Patterson." *Bulletin of Amer. Astron. Soc.* **37**, 1155.

Number	Name	λ	β	Period	λ	β	Period	a/b ratio	a/c ratio
1164	Kobolda	**270°**	**-61°**	**4.141699 h**				**1.5**	**1.4**
1413	Roucarie	**122°**	**10°**	**6.530557 h**	311°	37°	6.530558 h	**1.5**	**1.7**
1998	Titius	**236°**	**2°**	**6.126051 h**	54°	16°	6.126052 h	**1.2**	**2.4**
2233	Kuznetsov	**13°**	**8°**	**5.029548 h**	192°	1°	5.029547 h	**1.2**	**1.3**
2511	Patterson	**215°**	**-80°**	**4.140798 h**	64°	-81°	4.140797 h	**1.7**	**2.8**
3198	Wallonia	**115°**	**-47°**	**7.565854 h**	253°	-45°	7.565858 h	**1.4**	**1.7**
5040	Rabinowitz	**101°**	**48°**	**4.690155 h**				**1.1**	**1.8**
5096	Luzin	**75°**	**54°**	**3.054594 h**	249°	35°	3.054594 h	**1.4**	**1.8**

Table IV. Results of Pole/Shape modeling. The preferred solution is listed first in bold text.

Kaasalainen, M.; Torppa, J. (2001). "Optimization Methods for Asteroid Lightcurve Inversion. I. Shape Determination." *Icarus* **153**, 24-36.

Kaasalainen, M.; Torppa J.; Muinonen, K. (2001). "Optimization Methods for Asteroid Lightcurve Inversion. II. The Complete Inverse Problem." *Icarus* **153**, 37-51.

Klinglesmith III, D.A.; Hanowell, J.; Risley, E.; Turk, J.; Vargas, A.; Warren, C.A. (2013). "Asteroid Synodic Periods from Etscorn Campus Observatory." *Minor Planet Bull.* **40**, 65-67.

Malcolm, G. (2001). "Rotational Periods and Lightcurves of 1166 Sakuntala and 1568 Aisleen." *Minor Planet Bull.* **28**, 64.

Marciniak, A.; Pilcher, F.; Oszkiewicz, D.; Bartczak, P.; Santana-Ros, T.; Kamiński, K.; Urakawa, S.; Ogłoza, W.; Fauvaud, S.; Kankiewicz, P.; Kudak, V.; Żejmo, M.; Nishiyama, K.; Okumura, S.; Nimura, T.; Hirsch, R.; Konstanciak, I.; Tychoniec, Ł.; Figas, M. (2016) "Difficult cases in photometric studies of asteroids." *Proceedings of the Polish Astronomical Society* **3**, 84-87.

McNeill, A.; Mommert, M.; Trilling, D.E.; Llama, J.; Skiff, B. (2020). "Asteroid Photometry from the Transiting Exoplanet Survey Satellite: A Pilot Study." *Ap. J.* **245**, A29.

Oey, J.; Williams, H.; Groom, R.; Pray, D.; Benishek, V. (2017). "Lightcurve Analysis of Binary and Potential Binary Asteroids in 2015." *Minor Planet Bull.* **44**, 193-199.

Owings, L. (2013). "Lightcurves for 1896 Beer, 2574 Ladoga, 3301 Jansje, 3339 Treshnikov 3833 Calingasta, 3899 Wichterle, 4106 Nada, 4801 Ohre, 4808 Ballaero, and (8487) 1989 SQ." *Minor Planet Bull.* **40**, 8-10.

Pál, A.; Szakáts, R.; Kiss, C.; Bódi, A.; Bognár, Z.; Kalup, C.; Kiss, L.L.; Marton, G.; Molnár, L.; Plachy, E.; Sárneczky, K.; Szabó, G.M.; Szabó, R. (2020). "Solar System Objects Observed with TESS - First Data Release: Bright Main-belt and Trojan Asteroids from the Southern Survey." *Ap. J.* **247**, A26.

Pilcher, F. (2014). "New Photometric Observations of 279 Thule." *Minor Planet Bull*. **41**, 73-75.

Pilcher, F.; Franco, L.; Pravec, P. (2017). "319 Leona and 341 California - Two Very Slowly Rotating Asteroids." *Minor Planet Bull*. **44**, 87-90.

Polakis, T.; Skiff, B.A. (2017). "Lightcurve Analysis for 341 California, 594 Mireille, 1115 Sabauda 1504 Lappeenranta, and 1926 Demiddelaer." *Minor Planet Bull*. **44**, 299-302.

Pravec, P.; Harris, A.W.; Scheirich, P.; Kušnirák, P.; Šarounová, L.; Hergenrother, C.W.; Mottola, S.; Hicks, M.D.; Masi, G.; Krugly, Yu.N.; Shevchenko, V.G.; Nolan, M.C.; Howell, E.S.; Kaasalainen, M.; Galád, A.; Brown, P.; Degraff, D.R.; Lambert, J.V.; Cooney, W.R.; Foglia, S. (2005). "Tumbling asteroids." *Icarus* **173**, 108-131.

Pravec, P.; Wolf, M.; Sarounova, L. (2008web, 2010web, 2013web). *http://www.asu.cas.cz/~ppravec/neo.htm*

Pravec, P.; Scheirich, P.; Durech, J.; Pollock, J.; Kusnirak, P.; Hornoch, K.; Galad, A.; Vokrouhlicky, D.; Harris, A.W.; Jehin, E.; Manfroid, J.; Opitom, C.; Gillon, M.; Colas, F.; Oey, J.; Vrastil, J.; Reichart, D.; Ivarsen, K.; Haislip, J.; LaCluyze, A. (2014). "The tumbling state of (99942) Apophis." *Icarus* **233**, 48-60.

Pray, D.P.; Galad, A.; Husarik, M.; Oey, J. (2008). "Lightcurve Analysis of Fourteen Asteroids." *Minor Planet Bull*. **35**, 34-36.

Satō, I.; Hamanowa, H.; Tomioka, H.; Uehara, S. (2015). "Possible Duplicities of Five Asteroids." *Intl J. Astr. Ap.* **5**, 193-207.

Sauppe, J.; Torno, S.; Lemke-Oliver, R.; Ditteon, R. (2007). "Asteroid Lightcurve Analysis at the Oakley Observatory - March/April 2007." *Minor Planet Bull.* **34**, 119-122.

Skiff, B.A.; McLelland, K.P.; Sanborn, J.J.; Pravec, P.; Koehn, B.W. (2019). "Lowell Observatory Near-Earth Asteroid Photometric Survey (NEAPS): Paper 3." *Minor Planet Bull.* **43**, 52-56.

Stephens, R.D. (2015). "Asteroids Observed from CS3: 2015 January - March." *Minor Planet Bull.* **42**, 200-203.

Stephens, R.D. (2016). "Asteroids Observed from CS3: 2015 July - September." *Minor Planet Bull.* **43**, 52-56.

Stephens, R. (2017). "Asteroids Observed from CS3: 2016 - September." *Minor Planet Bull*. **44**, 49-52.

Stephens, R. (2018). "Asteroids Observe from CS3: 2018 April - June." *Minor Planet Bull*. **45**, 353-355.

Stephens, R.D.; Coley, D. (2013). "A Plethora of Phocaea Asteroids." *Minor Planet Bull.* **40**, 203-204.

Stephens, R.D.; Coley, D.; Warner, B.D. (2014). "Collaborative Asteroid Lightcurve Analysis at the Center for Solar System Studies: 2013 April-June." *Minor Planet Bull.* **41**, 8-13.

Stephens, R.D.; Warner, B.D. (2019). "Main-belt Asteroids Observed from CS3: 2019 April to June." *Minor Planet Bull.* **46**, 449-456.

Stephens, R.D.; Warner, B.D. (2020a). "Main-belt Asteroids Observed from CS3: 2019 July to September." *Minor Planet Bull.* **47**, 50-60.

Stephens, R.D.; Warner, B.D. (2020b). "Main-Belt Asteroids Observed from CS3: 2019 October to December." *Minor Planet Bull.* **47**, 125-133.

Tonry, J.L.; Denneau, L.; Flewelling, H.; Heinze, A.N.; Onken, C.A.; Smartt, S.J.; Stalder, B.; Weiland, H.J.; Wolf, C. (2018). "The ATLAS All-Sky Stellar Reference Catalog." *Astrophys. J.* **867**, A105.

Warner, B.D. (2007). "Initial Results from a Dedicated H-G Project." *Minor Planet Bull*. **37**, 57-64.

Warner, B.D. (2008). "Asteroid Lightcurve Analysis at the Palmer Divide Observatory: February-May 2008." *Minor Planet Bull*. **35**, 163-166.

Warner, B.D. (2009). "Asteroid Lightcurve Analysis at the Palmer Divide Observatory: 2008 December - 2009 March." *Minor Planet Bull.* **36**, 109-116.

Warner, B.D. (2011). "Upon Further Review: V. An Examination of Previous Lightcurve Analysis from the Palmer Divide Observatory." *Minor Planet Bull.* **38**, 63-65.

Warner, B.D. (2012a). "Asteroid Lightcurve Analysis at the Palmer Divide Observatory: 2011 June - September." *Minor Planet Bull.* **39**, 16-21.

Warner, B.D. (2012b). "Asteroid Lightcurve Analysis at the Palmer Divide Observatory: 2011 September - December." *Minor Planet Bull.* **39**, 69-80.

Warner, B.D. (2014a). "Asteroid Lightcurve Analysis at CS3-Palmer Divide Station: 2014 March-June." *Minor Planet Bull.* **41**, 235-241.

Warner, B.D. (2014b). "Asteroid Lightcurve Analysis at CS3-Palmer Divide Station: 2014 June-October." *Minor Planet Bull.* **42**, 54-60.

Warner, B.D. (2015). "Asteroid Lightcurve Analysis at CS3-Palmer Divide Station: 2014 October-December." *Minor Planet Bull.* **42**, 108-114.

Warner, B.D. (2016). "Asteroid Lightcurve Analysis at CS3-Palmer Divide Station: 2016 April-July." *Minor Planet Bull.* **43**, 300-304.

Warner, B.D.; Harris, A.W.; Pravec, P. (2009). "The Asteroid Lightcurve Database." *Icarus* **202**, 134-146. Updated 2020 Oct. *http://www.minorplanet.info/lightcurvedatabase.html*

Warner, B.D.; Harris, A.W.; Coley, D.; Stephens, R.D.; Allen, B.; Higgins, D. (2010). "Lightcurve Analysis of 279 Thule." *Minor Planet Bull*. **37**, 168-169.

Waszczak, A.; Chang, C.-K.; Ofek, E.O.; Laher, R.; Masci, F.; Levitan, D.; Surace, J.; Cheng, Y.-C.; Ip, W.-H.; Kinoshita, D.; Helou, G.; Prince, T.A.; Kulkarni, S. (2015). "Asteroid Light Curves from the Palomar Transient Factory Survey: Rotation Periods and Phase Functions from Sparse Photometry." *Astron. J.* **150**, A75.

SPIN/SHAPE MODEL FOR 1164 Kobolda

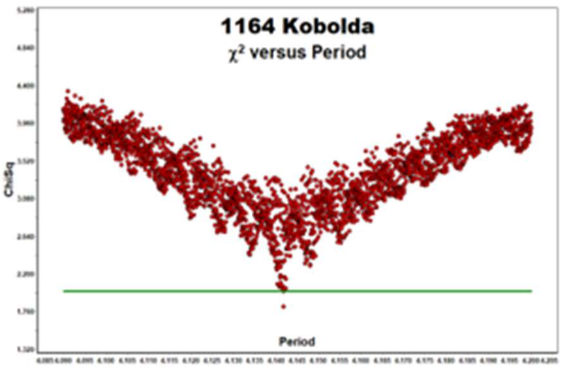

Figure 1. The initial period search results.

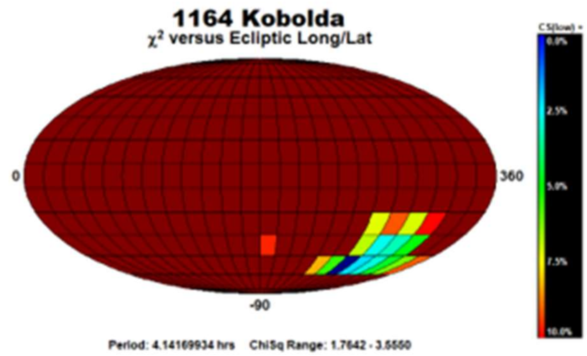

Figure 2. The pole search found two probable solutions.

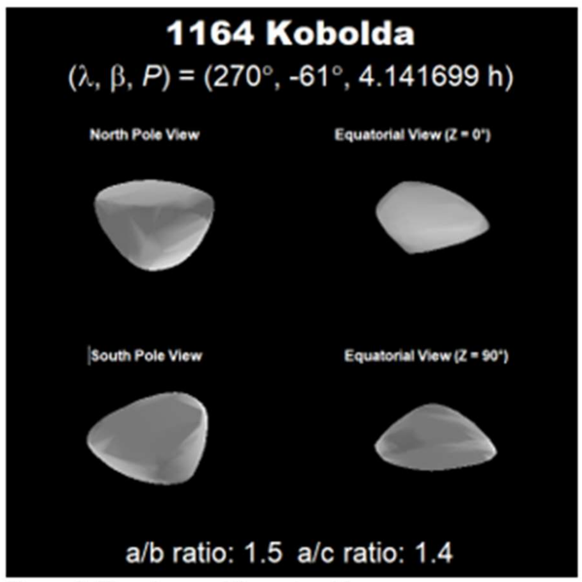

Figure 3. The shape of the asteroid.

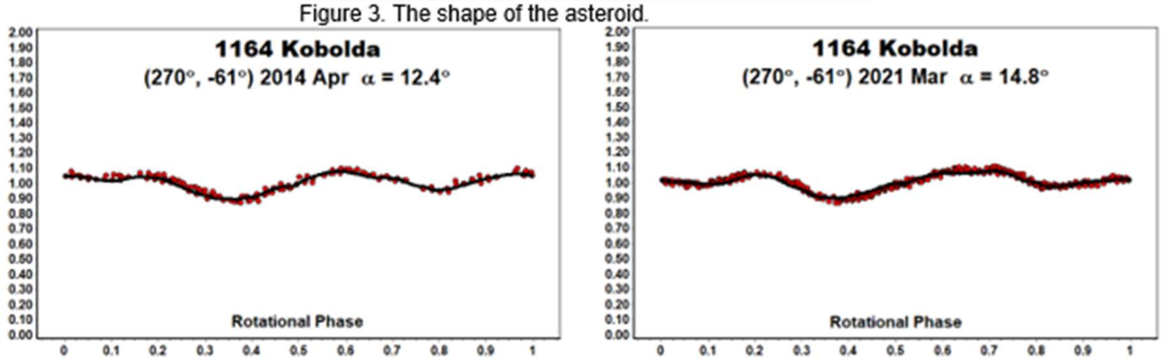

Figure 4/5. The comparison plots are against the preferred pole solution. The red dots indicate the data used for modeling while the black line is the smoothed lightcurve for generated by the shape at the time of the observations. The match is very close on both occasions, which gives confidence in the shape/spin axis model.

SPIN/SHAPE MODEL FOR 1413 Roucarie

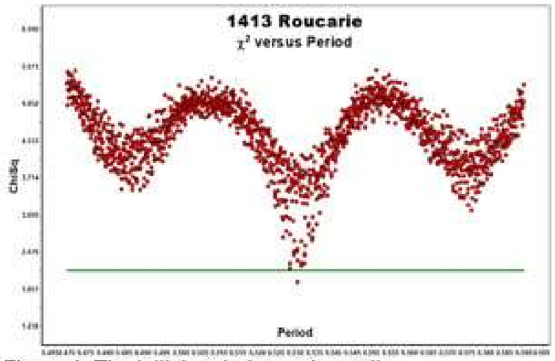

Figure 1. The initial period search results.

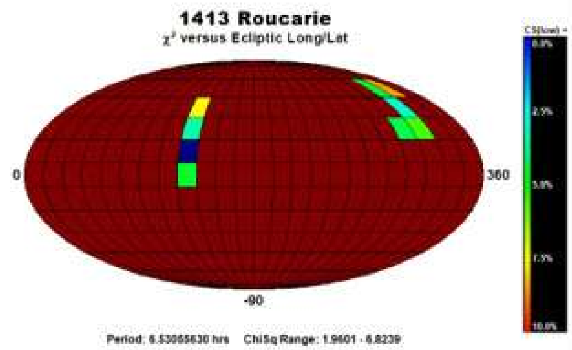

Figure 2. The pole search found two probable solutions.

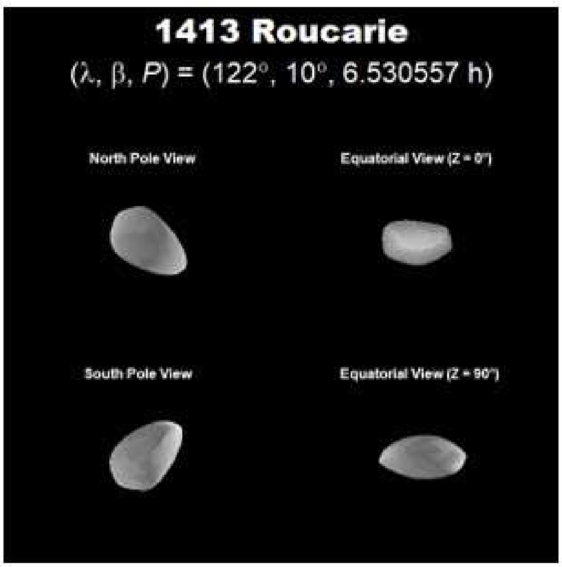

Figure 3. The shape of the asteroid based on the preferred solution.

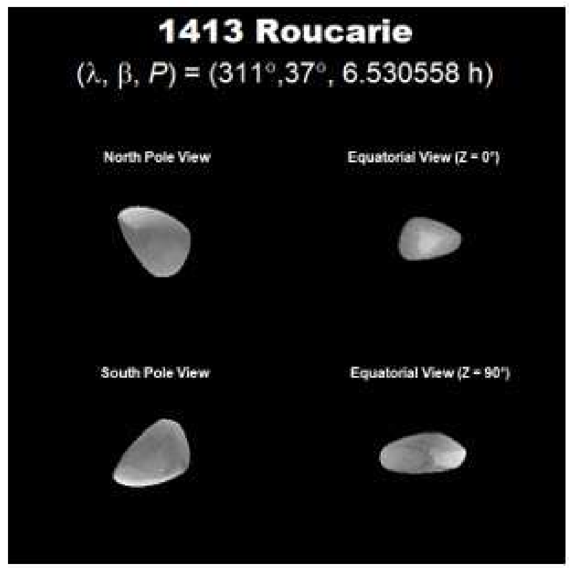

Figure 4. The shape of the asteroid based upon the secondary solution.

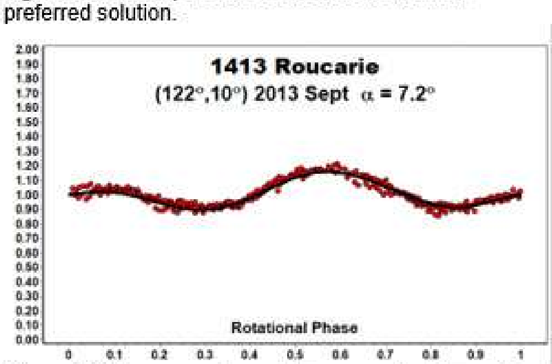

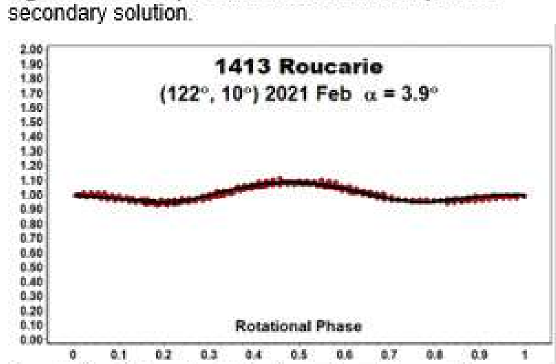

Figure 5/6. The comparison plots are against the preferred pole solution. The red dots indicate the data used for modeling while the black line is the smoothed lightcurve for generated by the shape at the time of the observations. The match is very close on both occasions, which gives confidence in the shape/spin axis model.

SPIN/SHAPE MODEL FOR 1998 Titius

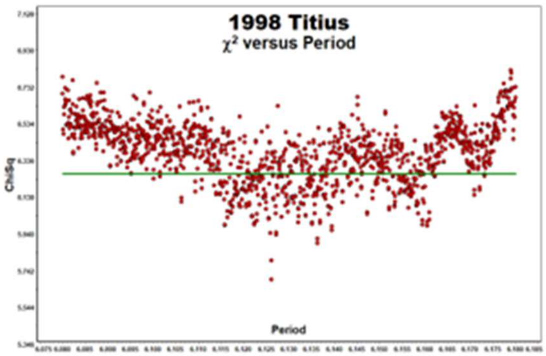

Figure 1. The initial period search results.

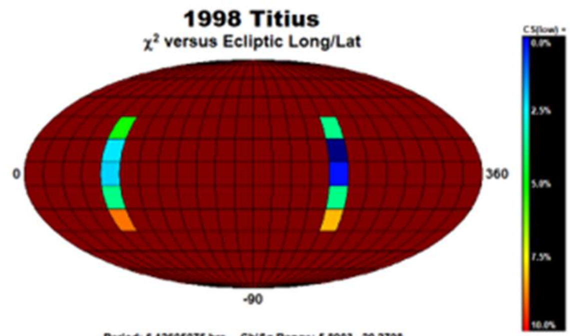

Figure 2. The pole search found two probable solutions.

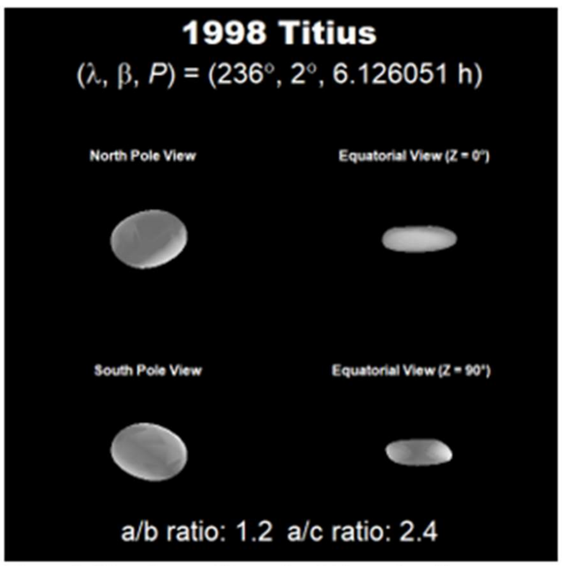

Figure 3. The shape of the asteroid based on the preferred solution.

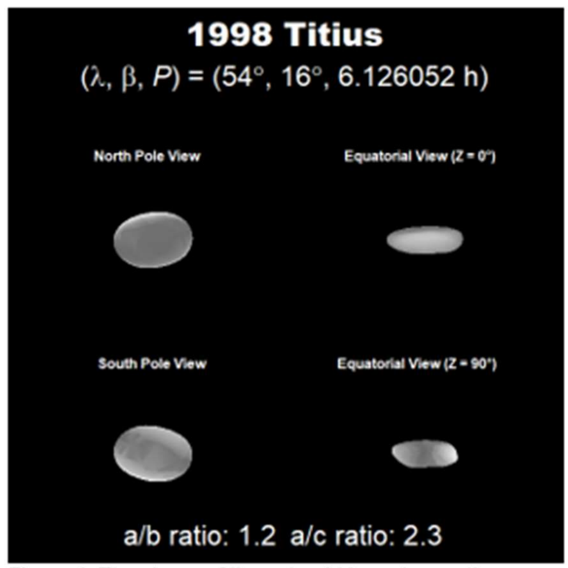

Figure 4. The shape of the asteroid based upon the secondary solution.

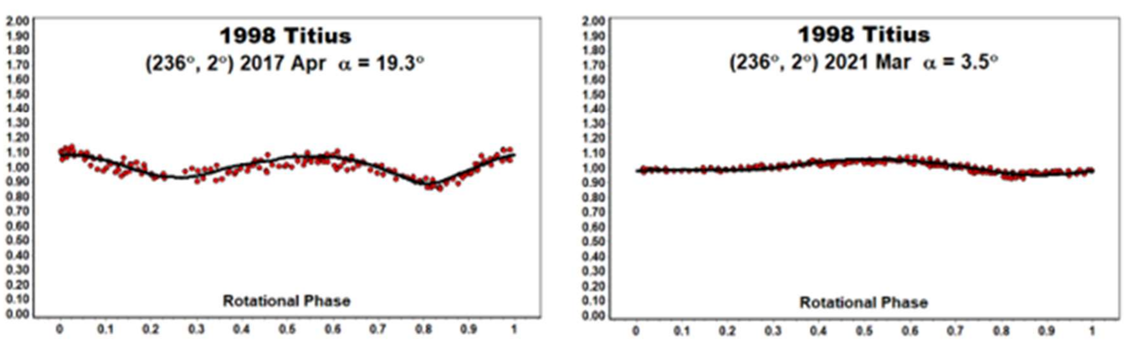

Figure 5/6. The comparison plots are against the preferred pole solution. The red dots indicate the data used for modeling while the black line is the smoothed lightcurve for generated by the shape at the time of the observations. The match is very close on both occasions, which gives confidence in the shape/spin axis model.

SPIN/SHAPE MODEL FOR 2233 Kuznetsov

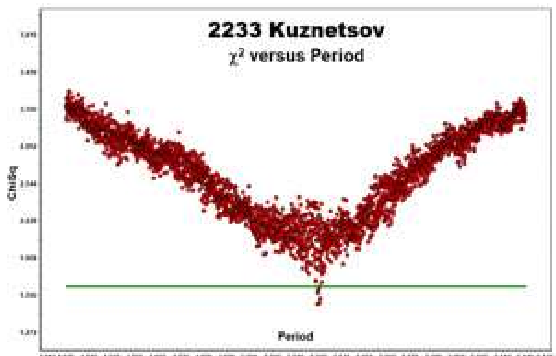

Figure 1. The initial period search results.

Figure 2. The pole search found two probable solutions.

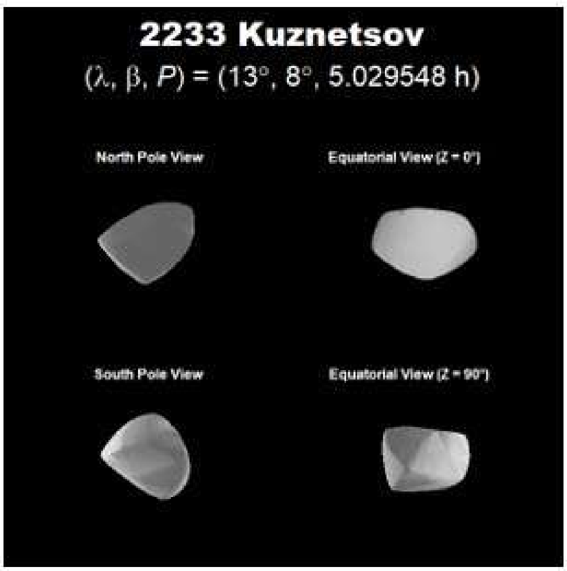

Figure 3. The shape of the asteroid based on the preferred solution.

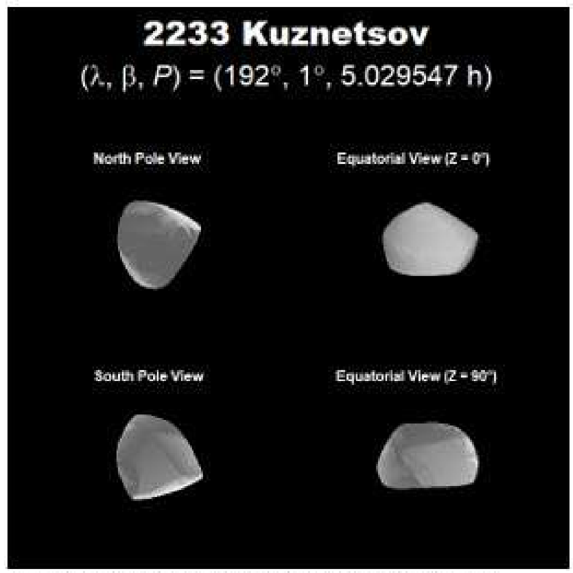

Figure 4. The shape of the asteroid based upon the secondary solution.

Figure 5/6. The comparison plots are against the preferred pole solution. The red dots indicate the data used for modeling while the black line is the smoothed lightcurve for generated by the shape at the time of the observations. The match is very close on both occasions, which gives confidence in the shape/spin axis model.

SPIN/SHAPE MODEL FOR 2511 Patterson

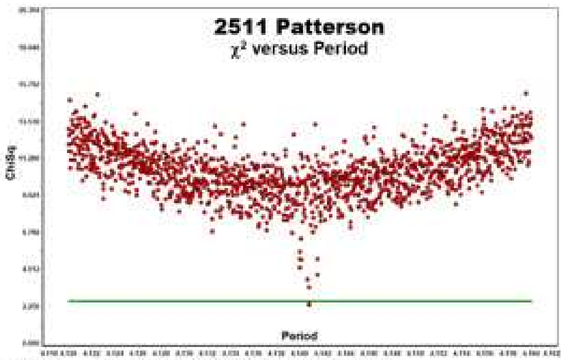

Figure 1. The initial period search results.

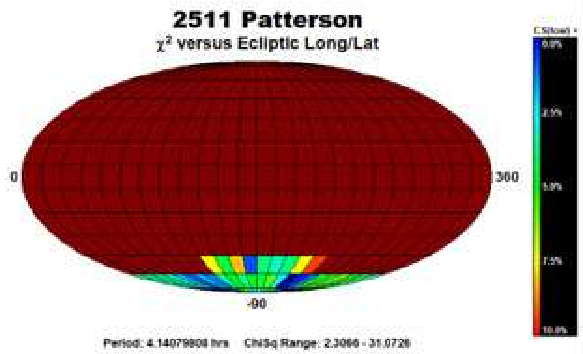

Figure 2. The pole search found two probable solutions.

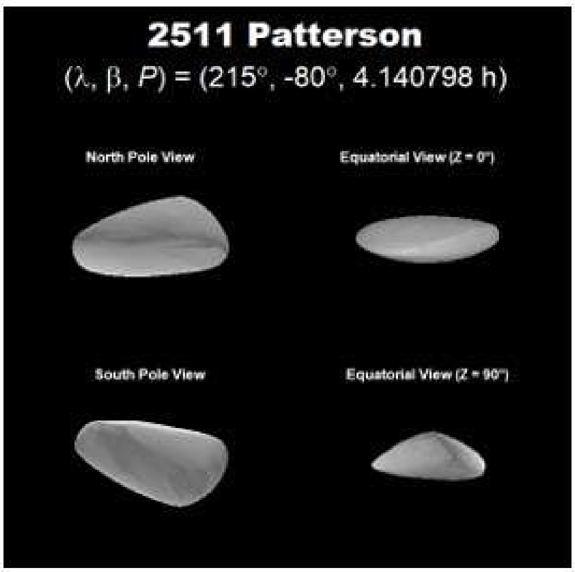

Figure 3. The shape of the asteroid based on the preferred solution.

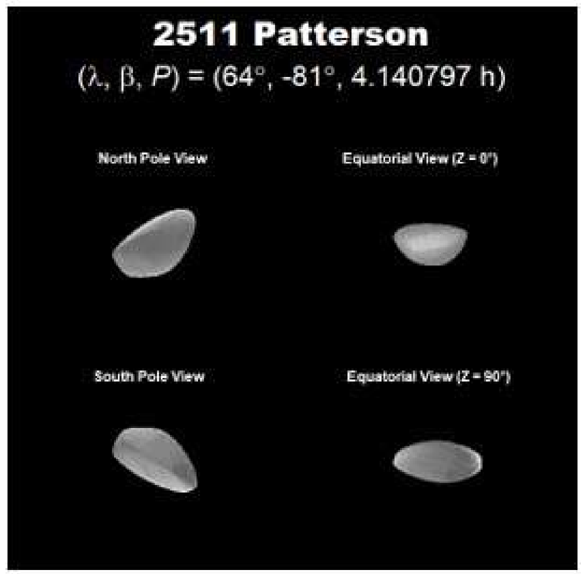

Figure 4. The shape of the asteroid based upon the secondary solution.

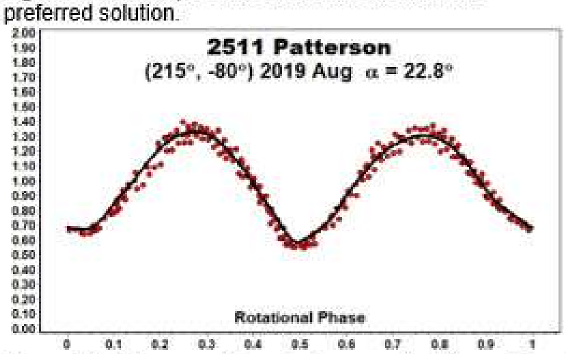

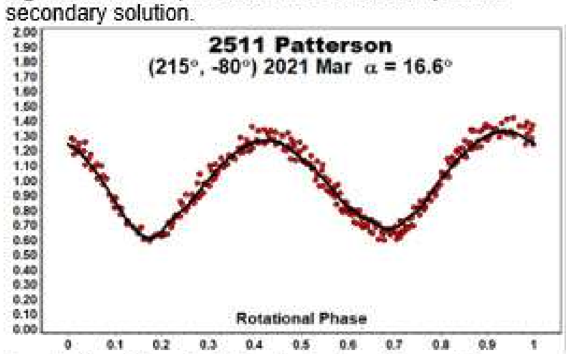

Figure 5/6. The comparison plots are against the preferred pole solution. The red dots indicate the data used for modeling while the black line is the smoothed lightcurve for generated by the shape at the time of the observations. The match is very close on both occasions, which gives confidence in the shape/spin axis model.

SPIN/SHAPE MODEL FOR 3198 Wallonia

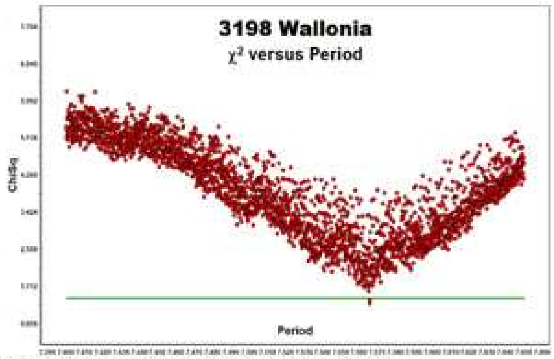

Figure 1. The initial period search results.

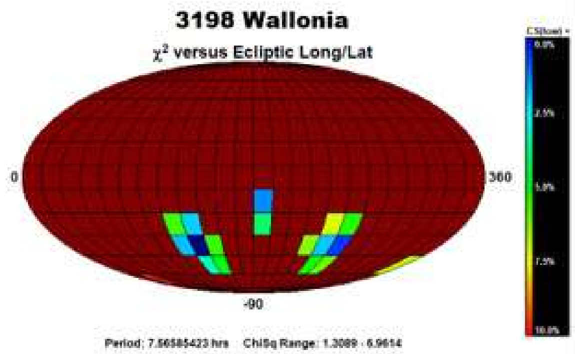

Figure 2. The pole search found two probable solutions.

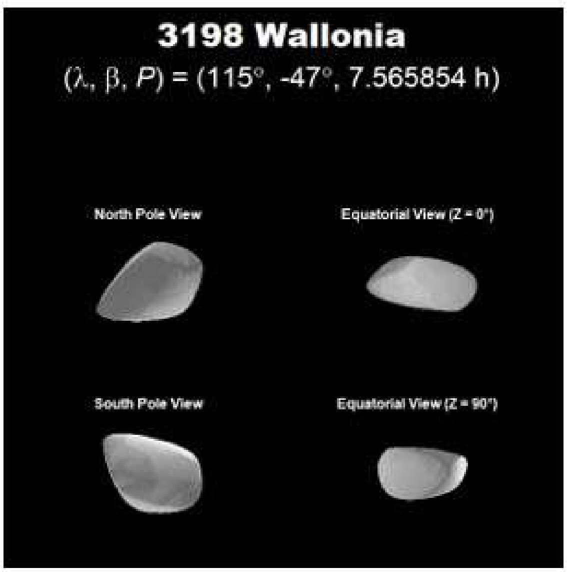

Figure 3. The shape of the asteroid based on the preferred solution.

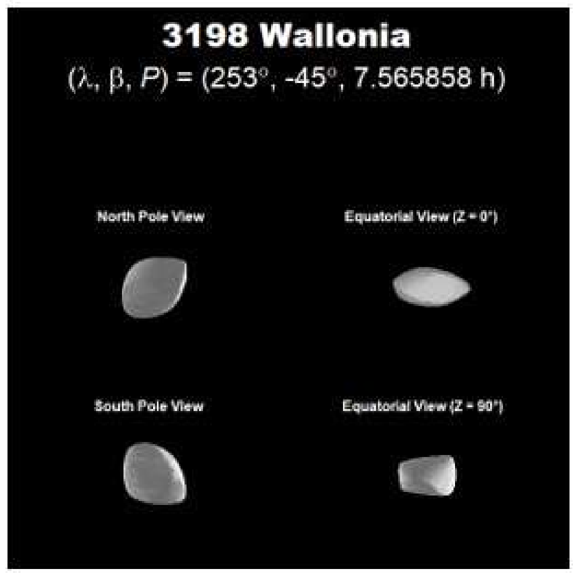

Figure 4. The shape of the asteroid based upon the secondary solution.

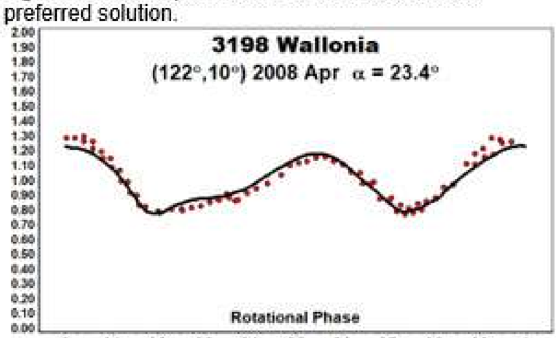

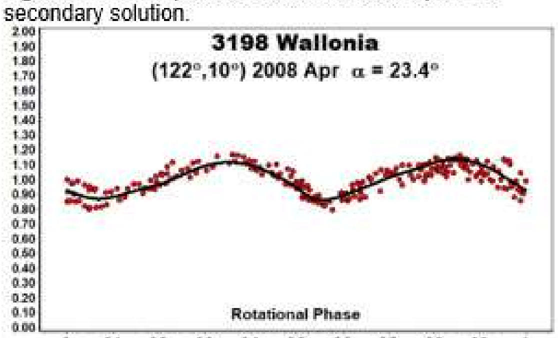

Figure 5/6. The comparison plots are against the preferred pole solution. The red dots indicate the data used for modeling while the black line is the smoothed lightcurve for generated by the shape at the time of the observations. The match is very close on both occasions, which gives confidence in the shape/spin axis model.

SPIN/SHAPE MODEL FOR 5040 Rabinowitz

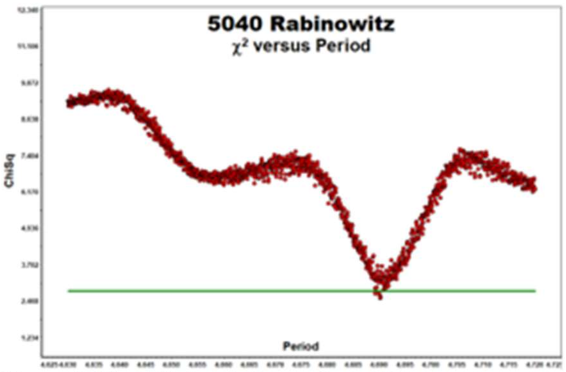

Figure 1. The initial period search results.

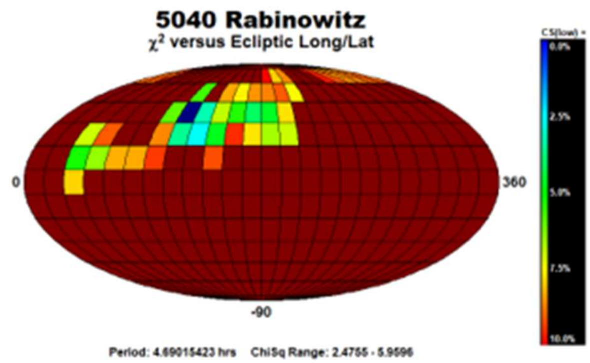

Figure 2. The pole search found two probable solutions.

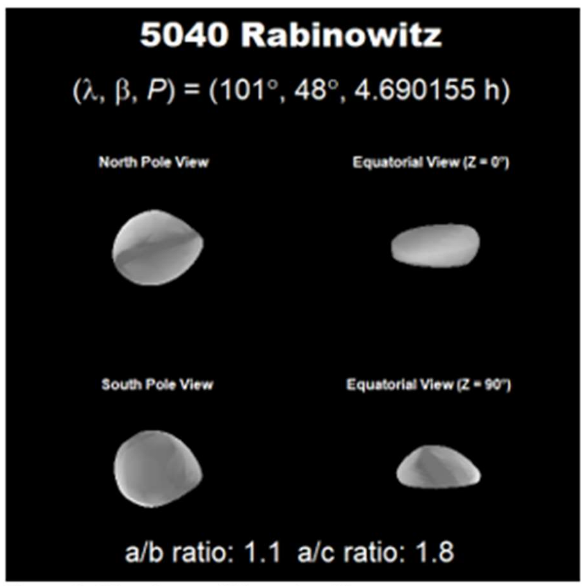

Figure 3. The shape of the asteroid.

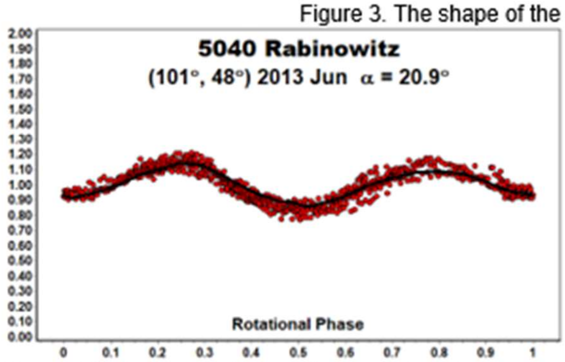

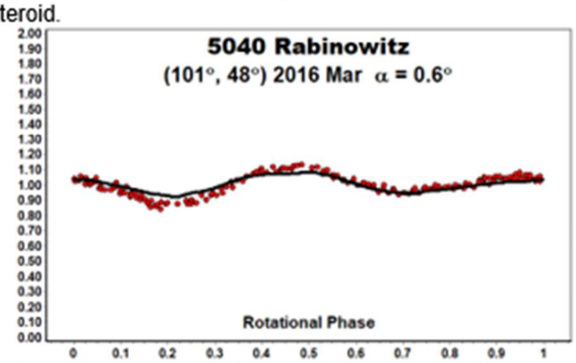

Figure 4/5. The comparison plots are against the preferred pole solution. The red dots indicate the data used for modeling while the black line is the smoothed lightcurve for generated by the shape at the time of the observations. The match is very close on both occasions, which gives confidence in the shape/spin axis model.

SPIN/SHAPE MODEL FOR 5096 Luzin

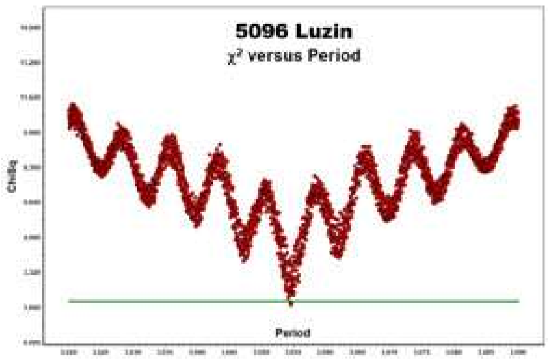

Figure 1. The initial period search results.

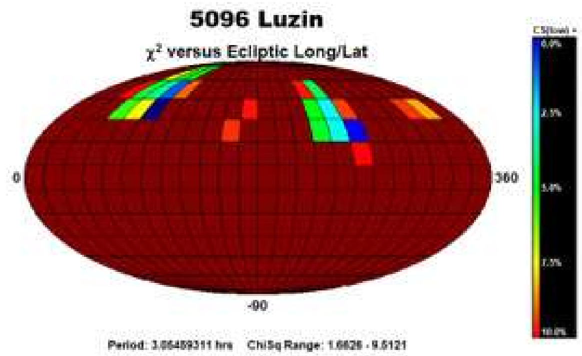

Figure 2. The pole search found two probable solutions.

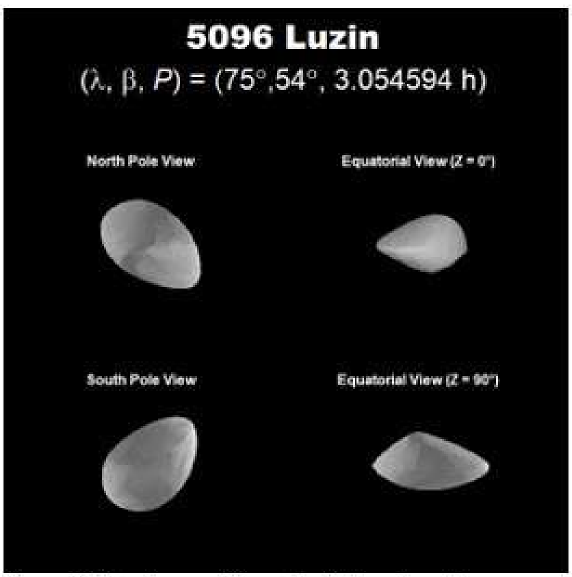

Figure 3. The shape of the asteroid based on the preferred solution.

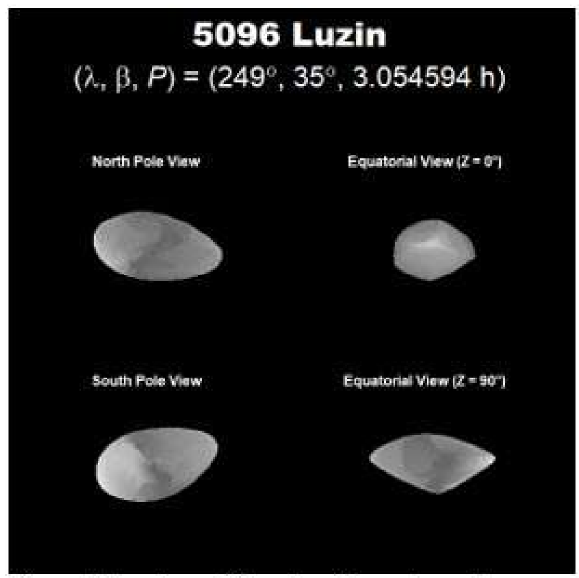

Figure 4. The shape of the asteroid based upon the secondary solution.

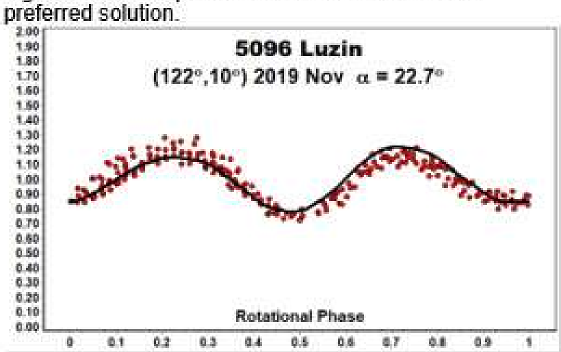

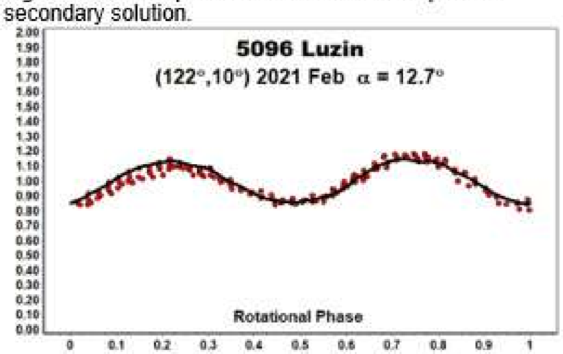

Figure 5/6. The comparison plots are against the preferred pole solution. The red dots indicate the data used for modeling while the black line is the smoothed lightcurve for generated by the shape at the time of the observations. The match is very close on both occasions, which gives confidence in the shape/spin axis model.